UNIVERSITY OF GAZİANTEP

GRADUATE SCHOOL OF

NATURAL & APPLIED SCIENCES

DESIGN OF THE OPTIMUM OGEE SPILLWAY TOE FOR A MAXIMUM ENERGY DISSIPATION

M. Sc. THESIS

IN

CIVIL ENGINEERING

BY

JEAN BAPTISTE MUMPUTU

SEPTEMBER, 2018

M.Sc. Thesis in Civil Engineering

JEAN BAPTISTE MUMPUTU

Design of the Optimum Ogee Spillway Toe for a Maximum Energy Dissipation

M.Sc. Thesis

in

Civil Engineering

University of Gaziantep

Supervisor

Associate Prof. Dr. Mehmet İshak YÜCE

By

Jean Baptiste MUMPUTU

September 2018

REPUBLIC OF TURKEY
UNIVERSITY OF GAZİANTEP
GRADUATE SCHOOL OF NATURAL & APPLIED SCIENCES
CIVIL ENGINEERING DEPARTMENT

Name of the thesis: Design of the Optimum Ogee Spillway Toe for a Maximum Energy Dissipation

Name of the student: Jean Baptiste MUMPUTU

Exam date: 17.09.2018

Approval of the graduate school of natural and applied science.

Prof. Dr. Ahmet Necmeddin YAZICI
Director

I certify that this thesis satisfies all the requirements as a thesis for the degree of Master of Science.

Prof. Dr. Hanifi ÇANAKÇI
Head of Department

This is to certify that we have read this thesis and that in our consensus opinion it is fully adequate, in scope and quality, as a thesis for the degree of Master of Science.

Associate Prof. Dr. Mehmet İshak YÜCE
Supervisor

Examining Committee Members:	Signature
Prof. Dr. Mehmet ÜNSAL	…………
Prof.Dr. Hanifi ÇANAKCI	…………
Associate Prof. Dr. Mehmet İshak YÜCE	…………

I hereby declare that all information in this document has obtained and presented in accordance with academic rules and ethical conduct. I also declare that, as required by these rules and conduct, I have fully cited and referenced all material and results that are not original to this work.

Jean Baptiste MUMPUTU

ABSTRACT

DESIGN OF THE OPTIMUM OGEE SPILLWAY TOE FOR A MAXIMUM ENERGY DISSIPATION
JEAN BAPTISTE MUMPUTU

M.Sc. in Civil Engineering
Supervisor: Associate Prof. Dr. Mehmet İshak YÜCE
September 2018
53 pages

Hydraulic design of a spillway has been one of the most studied subjects in hydraulic engineering. Properly designed, flow condition dependent spillways will be able to release water efficiently and safely from a dam reservoir to the downstream. This study aims to investigate the energy dissipation at the toe of ogee spillway by making an ogee spillway with different end sill models at the downstream by using a commercially available Flow-3D. The case A model was an ogee spillway with rectangular end sill, the case B, C, D and E with a curved end sill with radius of 0.10, 0.15, 0.18 and 0.20 meters, respectively, and the case F which has an inclined end sill. The major amount of energy dissipation occurs at the toe in the region where the hydraulic jump takes place. The hydraulic jump is used to dissipate energy at the downstream. These models were compared to one another to see the corresponding energy loss respectively. To simulate the turbulent flow, the "$k-\varepsilon$" turbulence model is done in the numerical modelling.

The numerical result shows that the model with curved end sill dissipates more energy than others. In the case F model with inclined end sill, it can be concluded that the hydraulic jump did not occur, the velocity remained high for all cases of discharge and the energy loss is insignificant regarding its form. Therefore, energy loss changes in relation to discharge, most loss occurs at low discharge while in the case of high discharges energy loss decreases. Results indicated numerical methods as convenient and time-saving, with least errors.

Keywords: Ogee spillway, Energy dissipation, Flow-3D, Numerical modeling

ÖZET

ENERJİ KIRIMI İÇİN OPTİMUM DOLUSAVAK UCU TASARIMI
JEAN BAPTİSTE MUMPUTU

Yüksek Lisans Tezi, İnşaat Mühendisliği Bölümü
Danışman: Doç. Dr. Mehmet İshak YÜCE
Eylül 2018
53 sayfa

Bir dolusavakın tasarımı, hidrolik mühendisliğinde en çok çalışılan konulardan biri olmuştur. Düzgün tasarlanan dolusavaklar suyu bir baraj gölünden nehir yatağına kadar verimli ve güvenli bir şekilde serbest bırakabileceklerdir. Bu çalışma, ticari olarak mevcut Flow-3D programi kullanarak, mansapta farklı son eşik modelleri ile farklı bir merdane dolusavak modelleri oluşturarak, ogee döküntüsünün burnundaki enerji yayılımını araştırmayı amaçlamaktadır. A modeli dikdörtgen uç eşikli, B, C, D ve E modelleri ile 0.10, 0.15, 0.18 ve 0.20 metrelik yarıçaplı eğimli uç eşik ve eğimli bir uç eşik olan F modeli analiz edilmiştir. Hidrolik sıçramanın gerçekleştiği bölgedeki büyük enerji kaybı miktarı ayaktadır. Hidrolik sıçrama, aşağı akıştaki enerjiyi dağıtmak için kullanılır. Bu modellerin her birinde meydana gelen enerji kaybını oranları karşılaştırıldı. Türbülanslı akışı simüle etmek için “$k - \varepsilon$” modeli kullannıldı.

Sayısal sonuç, eğik uç eşikli ikinci modelin diğerlerine göre daha fazla enerji yaydığını göstermektedir. Eğik uç eşikli F modelinde, hidrolik sıçramanın gerçekleşmediği, tüm akıntı durumları için hızın yüksek kaldığı ve enerji kaybının önemsiz derecede olduğu sonucuna varılabilir. Debiye bağlı olarak enerji kaybı değişmekte, düşük debilerde yüksek oranda enerji kaybı meydana gelirken, yüksek debilerde enerji kaybı oranı azalmaktadır. Sonuçlar sayısal yöntemler için uygun ve zaman tasarruflu, en az hata ile belirtildi.

Anahtar Kelimeler: Ogee dolusavağı, Enerji dağılımı, Akış-3D, Sayısal modelleme

To

My Parents

ACKNOWLEDGEMENT

I would like to thank to my supervisor Associate Prof. Dr. Mehmet İshak YÜCE**.** Dr. YUCE's door was always open whenever I ran into a trouble spot or had a question about my research or writing. He consistently allowed this study to be my own work, always providing insight and guiding me in the right direction. I am grateful and proudest to work under his academic guidance.

I must express my profound gratitude to my parents for providing me with unfailing support and continuous encouragement throughout my years of study and through the process of researching and writing this thesis. Also to my brothers and sisters without their passionate participation and input, the validation survey could not have been successfully conducted.

TABLE OF CONTENTS

Page

LISTS OF TABLES

Page

LIST OF FIGURES

Page

LIST OF SYMBOLS/ABBREVIATIONS

USBR	United States Bureau of Reclamation
CFD	Computational Fluid Dynamics
USACE	United States army corps of engineers
WES	Waterway experimental section
AASHTO	American Association of State Highway and Transportation officials
Hd	Design head
G	Gravity
R	Radius
Q	Discharge
H	Head
L	Effective length of crest
L'	Net length of crest
V	Velocity
VOF	Volume of fluid
FAVOR	Fractional Area / Volume Obstacle Representation
ρ	Density of water
ν	Viscosity
f	Force
a	Acceleration
FSL	Full supply level
VF	Volume Fraction
PDE	Partial Differential Equation
H_e	Total head over the crest.
H_a	Velocity head
STL	Stereolithography

CHAPTER 1

INTRODUCTION

1.1 General Background

Rapid population growth with the associated need for water supply, flood control, hydroelectric generation, recreation, navigation and fishing has made construction of dams a necessity throughout the world. Water is amongst the most important natural resources for the survival of mankind; its preservation is of the utmost importance. Technological improvements in the design and analysis of dams require a better management of water resources.

In hydraulic engineering, one of the most important issues is the safety of flood discharging and energy dissipation, especially in cases of high water head and large unit discharge. If their capacities are less than the difference between inflows and outflows, they might overflow and cause the overtopping problem. The most sensitive structures which can be fall by a small overtopping are Earth-fill dams (Hager, 1985; Ohtsu et al., 1999; Rajaratnam and Subramanya, 1968). This highlights that all hydraulic structures should have its own design conditions such as adequate capacity, depth and stability to ensure that the outlet design can admit the flow velocity and energy of water flowing from upstream. Some sort of energy dissipating structures required to prevent deterioration of the downstream channels. The design could vary from arrangement of multiple basins to a simple headwall, depending on the number and size of ducts involved the resistance of the exit channel bed material against erosion, the frequency and the intensity of flow discharge. Dissipation of energy is closely associated with spillway design, flow discharge, the difference between upstream and downstream water levels. It is worth noting that the discharge of water over a spillway to the downstream, flow transits into the supercritical flow condition and then a hydraulic jump may take place. It is preferable to consider the energy dissipation process stages, some of which may be combined or separated. The required type of energy dissipator is sometimes determined by environmental factors. The reason being that dissipators can affect th environment adversely, for example; deep-seated stilling basins with highly aerated flows inducing nitrogen supersaturation which would not be permissible where fish life is an important consideration (Khatsuria, 2005).

In this study, we briefly review the broad perspectives that have shaped the direction of thinking about ogee spillways with an S-shaped profile. They are the most commonly used spillways due to their proper function, ability to control floodwater and high safety factor (Daneshkhah and Vosoughifar, 2012; Yuce et al. 2015). Researchers have studied physical model experiments deriving empirical formulae to understand the flow mechanism over hydraulic structures. With recent advances in computational and numerical techniques, new tools are being used to solve problems involving fluid flow. Based on its faster and more economical solutions than physical models, engineers are interested to improve the capability of Computational Fluid Dynamics (CFD) software (Chanel, 2008). The CFD numerical simulation techniques have been progressively accepted by the Hydraulic engineering community not only as an investigative tool in the research institutions (Kjellesvig, 1996; Savage and Johnson, 2001) but also as a useful design tool (Gessler, 2005). At the present research, the energy dissipation was investigated at the toe of ogee spillways with three different end sill models by employing a commercially available CFD program.

Some recent works show the capability of the CFD method in the numerical modeling of flow over several spillways. Johnson and Savage (2006) modeled an ogee-crested spillway by using Flow-3D software and compared the numerical results with physical measurements. Likewise Bombardelli et al. (2011) achieved satisfactory results by employing CFD software which is based on the Eulerian mesh dependent method. In addition to this, there are other benefits of using CFD methods in order to solve the early problematic flow characteristics for prototype cases, despite of significant lack of calibration and validation studies compared to physical modelling (ICOLD, 2012).

1.2 Spillways

A spillway is considered as one of the most important structures of a dam. It releases the flood wave from the reservoir to the downstream. By discharging water downstream, it comes with a high velocity that should be expended. This high kinetic energy flow may cause a serious problem on the channel bed (scour, damage, etc.). In order to avoid these problems, spillways should be controlled at the toe to safely function during the lifetime of the dam. In some cases, energy dissipaters are used along the slope to reduce the amount of space needed to effectively evacuate the flow without compromising the dam (USBR, 1973). It is worthwhile bearing in mind that, for the safety of all dams, the spillway capacity is primordial, particularly earthfill and rock-fill dams.

1.3 Spillway Classification

Classification of spillways can be based on various factors; functions, control structure and others features. Spillways are mostly called "controlled or uncontrolled, relying on whether they are gated or ungated. They are generally classified as; Ogee, Chute, Side channel, Shaft, Siphon, Straight drop or over fall, Tunnel /Culvert, Labyrinth and Stepped (Russell, 2005; Vischer et al, 1988).

1.3.1 Ogee (overflow) Spillway

In this study, an uncontrolled ogee spillway is used in the analyses. An ogee spillway is an improvement upon the free overfall and it is used with almost all types of dams. The nappe-shaped ogee spillways are the most common types because of their efficient discharge. They are gravity structures that should be strong and have a solid foundation. The spillways are usually located in the main river channel. Three-zones can be distinguished on these spillways; the crest, the face and the toe.

Figure 1.2 View of an Ogee Spillway

1.4 Objective of Study

The study aims to examine and compare the rate of energy dissipation on an Ogee spillway with various end sill shapes. The performance of each shape was judged according to the dissipated energy, over a range of discharges.

The specific objectives of the study are:

- To numerically analyse and compare an ogee spillway model with different end sill shapes, then evaluate the rate of energy dissipation with a number of discharges.
- To determine the suitable shape that dissipates more energy than others.

1.5 Thesis Layout and Chapter Overview

This research is subdivided into five chapters as stated below:

The first chapter, namely introduction, provides a general background of this research, basics of spillways, classification of spillways, objectives and thesis layout. Briefly, it represents the framework of the research.

Chapter two contains literature review with previous studies performed on spillways, description of energy dissipation and background of numerical method.

Chapter three describes the research methodology used in this thesis, geometry description of different models with the development of the numerical model.

Chapter four consists of results and discussions and their interpretations. Finally, chapter five summarizes the conclusions and recommendations for future research.

CHAPTER 2

LITERATURE REVIEW

2.1 General

This chapter presents a brief review of the studies conducted in energy dissipation aspects of spillways and numerical models. The ogee spillway finds its extensive applications in hydraulic and environmental engineering, which is used to dissipate the energy of released flood wave. In a significant amount of the available literature on numerical analyses of spillways, Flow-3D is utilised, which allows the model to include only the water portion of the flow (Volume of flow method) and fully structured computational grid (Fractional Area/Volume Obstacle Representation method).

Sharif and Ravori (2014) evaluated the energy dissipation with Flow-3D by making three different buckets, the first model has a lip angle of 40 degrees and the two others were a compound bucket with different lip angle in each part; one of them has 20, 40 degree angles and another 40, 80 degrees. The major dissipation of energy occurred in the region where the jet plunged into the tailwater and the hydraulic sequent depth is used to evaluate the energy loss at downstream. They found that the numerical results were generally in correspondence with physical data. Asaram et al. (2016) studied the effects of different slopes over ogee spillway surface for energy dissipation. He made three ogee spillway models with slopes of 1:1, 0.85:1, and 0.75:1. The test was carried out in the laboratory to investigate the energy dissipation downstream of these models. The results of this study show that; while for the minimum depth relative energy losses were 67%, 65.03% and 67.20% for slopes of 1:1, 0.85:1 and 0.75:1 respectively, for the maximum depth the losses were 87.17%, 85% and 85.20%. He concluded that the height of jump depends on the slope of the spillway surface.

Morovati et al. (2016) investigated energy dissipation of pooled stepped spillways and discharge on flow pattern. The result obtained in numerical simulation (Flow 3D) was compared with experimental data. The comparison indicated that a decrease in the number of the steps of pooled stepped spillways reduces the velocity of flow at the end of the spillways. Moreover, the value of the turbulent kinetic energy was increased by the discharge value.

Kumcu, (2017) carried out a study of flow over spillway modeling, discharge rating curves, velocity patterns and pressures by using Flow-3D; his purpose was to compare the results of the physical model and the numerical model. A reasonable agreement between physical and numerical models in flow characteristics was found.

2.2 Spillway Toe

Spillway toe is the junction between the discharge channel and the energy dissipator. It is used to guide the flow of water passing down the spillway. A toe curve can be in circular arc form, tangential to both the rear slope and the apron (Figure 2.1). The design of its radius as a curve should be such that the excessive velocity flow can change its direction smoothly without hurdling. The minimum radius of the toe curvature should not be less than three times of the depth of flow entering the toe (Khatsura, 2005).

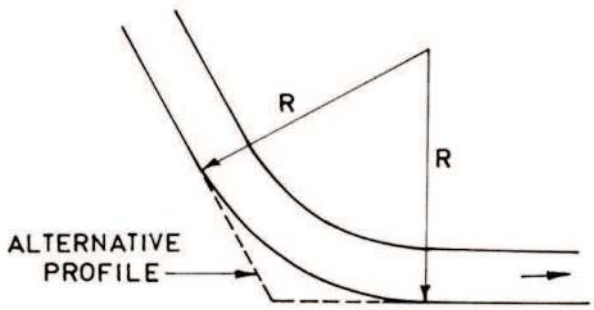

Figure 2.1 the curve of the toe at the base of the spillway

2.3 Discharge Characteristics

Generally, the discharge of water passing over an overflow spillway is calculated by:

$$Q = CL_eH_e^{3/2} \quad (2.1)$$

where Q is the discharge (m^3s^{-1}), L_e is effective length of the spillway crest (m), C is the discharge coefficient and H_e is the total head over the crest (m). If Q is the design discharge (Equation 2.1), then H_e is related to the design head, H_d plus the velocity head, H_a which means $H_e = H_d + H_a$. For high ogee spillways, since the velocity head is very low and $H_e = H_a$

Most of the overflow has a high value of the discharge coefficient because of the shape of the spillway and this coefficient is variable. Numerous factors influence the coefficient; the inclination of the upstream face, the depth of approach, the relation of the actual crest shape to the ideal nappe shape and downstream submergence (USBR, 1987). When the shape of the crest is different from the ideal shape or the head is greater or smaller than the design head, the coefficient changes as well.

2.4 Energy Dissipator

The discharge of water over spillway acquires a lot of kinetic energy by the time it reaches near the toe due to the conversion of potential energy into kinetic energy. Precaution should be taken to avoid scour and erosion in the spillway. Those energy dissipators are provided to dissipate the huge amounts of energy before water enters the downstream channel. The design procedure presents the recommended design steps for energy dissipation (Figure 2.2) (AASHTO, 2014).

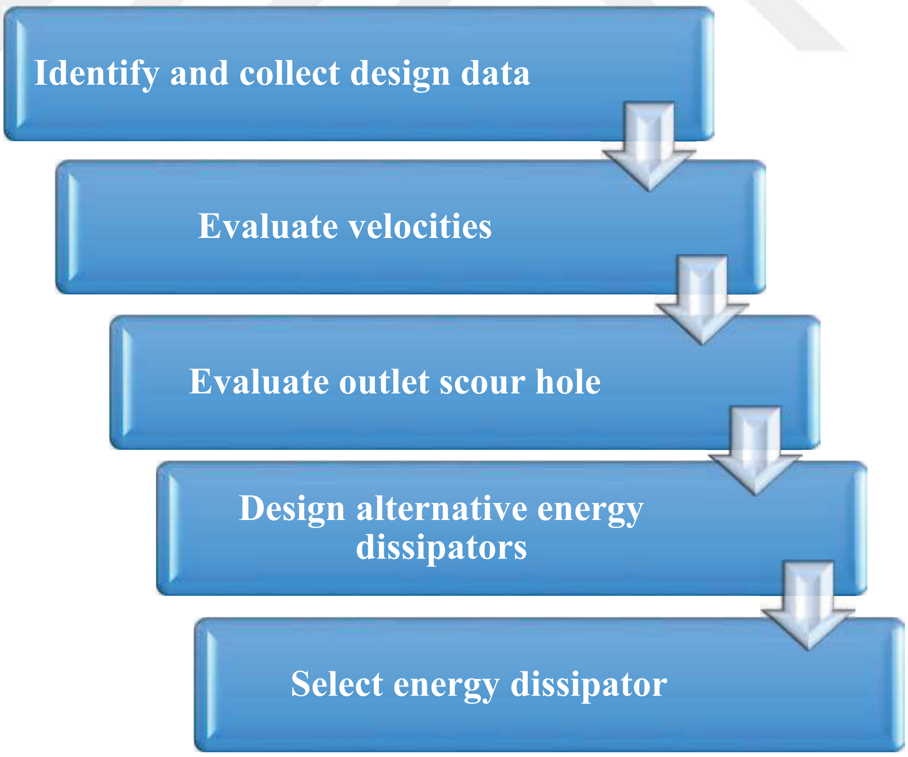

Figure 2.2 Energy Dissipater Design Procedures (AASHTO, 2014).

2.4.1 Types of Energy Dissipation Structures

There are a variety of dissipators that exist as outlet structures in spillway designs to dissipate energy, such as:

(a) ***Straight Drop***: this energy dissipator is particularly used in small drainage structures and low head spillways. Generally, the aerated free falling nappe in the straight drop produces supercritical flow on the apron. Furthermore, at downstream a hydraulic jump may occur.

(b) ***Stilling Basin***: the stilling basin has multiple forms and is used to dissipate the energy of water. This type of energy dissipation can be done by increasing the hydraulic jump within the basin. The location of the hydraulic jump should be known, in order to determine the length of the channel that requires protection.

In the hydraulic jump, the energy loss is computed by :

$$\Delta E = E_1 - E_2 = \frac{(y_2 - y_1)^2}{4 y_1 y_2} \tag{2.2}$$

where, ΔE is Energy loss in the jump, E_1= Energy at section 1, E_2= Energy at section 2, y_1= depth of water at section 1, and y_2= depth of water at section 2. The following devices may be incorporated in stilling basin design such as paved apron, chute blocks, baffle block and end sill that is the main subject of this thesis. Figure 2.5 shows various stilling basin type of energy dissipators.

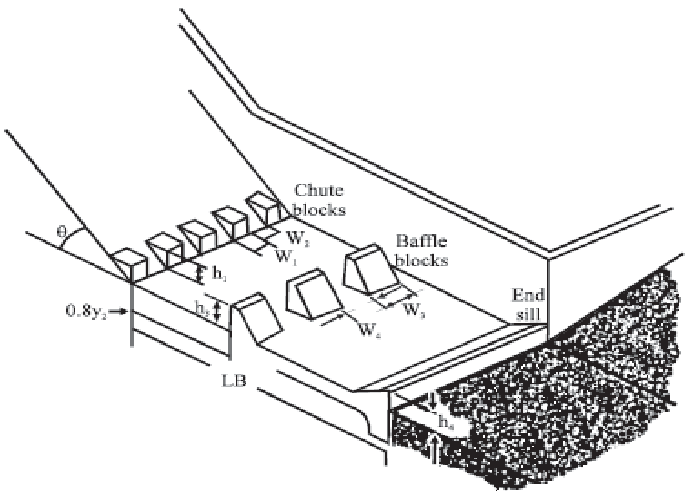

Figure 2.3 Stilling basin type of energy dissipators with chute and baffle blocks *(Federal Highway Administration, 1983)* USBR Type III Basin.

c) ***Flip Buckets***: This type is used when the downstream channel bed is relatively stable. The upward lip is designed to project the jet of water dozens of metres into the air, which dissipates part of its energy and prevents structural damage.

d) ***Roller Buckets***: this kind of energy dissipators are used when the tailwater level is higher than hydraulic jump basins.

e) ***Stepped Spillway***: another possibility to dissipate part of kinetic energy on the spillway face itself. An ogee stepped spillway is an ogee spillway with drops or steps, these steps reduce the speed of water by the time it flows downstream of the spillway before reaching the toe.

2.5 Numerical Methodology

The basic principles for all numerical models remain similar; the physical problems are represented by a set of partial differential equations (PDE). The flow of fluids are governed by the conservation of mass, momentum and energy . PDE system with series of algebraic equations can be substituted for Computational Fluid Dynamics (CFD) that can be solved by using numerical methods (Versteeg and Malalasekera, 2007). These equations are also known as Navier-Stokes equations (Wendet, 2009). Flow-3D is a CFD package that use finite volume method to solve Reynolds Averaged Navier-Stokes (RANS) equation, applying Fractional Area/Volume Obstacle Representation (FAVOR) technique to describe an obstacle (Flow science, 2012). In this study Flow-3D software has been used to evaluate the energy loss over spillways.

The equations 2.3 and 2.4 characterise continuity and RANS equations with FAVOR variables which are used for incompressible flows.

$$\frac{\partial}{\partial X_i}(u_i A_i) = 0 \tag{2.3}$$

$$\frac{\partial u_i}{\partial t} + \frac{1}{VF}\left(u_j\, A_j\, \frac{\partial u_i}{\partial x_j}\right) = \frac{1}{\rho}\frac{\partial p}{\partial x_i} + g_i + f_i \tag{2.4}$$

where, u_i is the velocity in x_i direction which are x, y, and z-directions; A_i is the fractional area open to flow in the subscript directions, VF is the volume fraction of fluid in each cell, t is the time, p is the hydrostatic pressure, ρ is the density, g_i is the gravitational force in subscript directions and f_i is the Reynolds stresses.

2.5.3 Volume of Fluid (Vof) Method

All elements do not have liquid when there is a free surface flow, part of the cells could be full and some other elements may be empty. Some cells with free surface could be partially filled. The practical way to identify the state of elements is to present a quantity F that records the fraction of volume of fluid (VOF) function. Several numerical methods are employed to solve free infinite boundaries in the different simulations in the recent years. The volume of fluid is a simple and powerful method created on the concept of a fractional intensity of fluid. Most studies have aproved the method to be more effective than others dealing with complex free boundary configurations.

Nichols and Hirt (1975) were the first to declare that Flow 3-D free surface is modeled by using VOF technology. There are three components that exist in VOF method; scheme of surface detection, an algorithm for tracking the surface as a clear interface moving through the computational grid and the application of boundary conditions to the surface. The fluid composition depends on VOF function F(x,y,z,t) (Nichols andHirt, 1981). The function shows the volume of flow per unit volume and satisfies the equations 2.7, 2.8 and 2.9.

$$\frac{\partial F}{\partial t}+\frac{1}{V_F}\left[\frac{\partial}{\partial x}(FA_{xu})+R\frac{\partial}{\partial y}\left(FA_{yv}\right)+\frac{\partial}{\partial z}(FA_{zw})+\xi\frac{FA_{xu}}{x}\right]=F_{DIF}+F_{SOR} \qquad (2.7)$$

$$F_{DIF}=\frac{1}{V_F}\{\frac{\partial}{\partial x}\left(v_F\,A_x\frac{\partial F}{\partial x}\right)+R\frac{\partial}{\partial x}\left(v_F\,A_y\,R\frac{\partial F}{\partial y}\right)+\frac{\partial}{\partial z}\left(v_F A_z\frac{\partial F}{\partial z}\right)+\xi\frac{v_F A_x F}{x}\} \qquad (2.8)$$

$$V_F\frac{\partial\rho}{\partial t}+\frac{\partial}{\partial x}(\rho u A_x)+R\frac{\partial}{\partial y}\left(\rho_v A_y\right)+\frac{\partial}{\partial z}(\rho_w A_z)+\xi\frac{\rho_u A_x}{x}=R_{DIF}+R_{SOR} \qquad (2.9)$$

where, ρ is the density of fluid, V_F is the fractional volume open to flow, R_{SOR} is the mass source and R_{DIF} is the term of turbulent diffusion. The velocity components (u,v,w) are in the coordinate directions (x,y,z) or (r, R_{SOR}, z). A_y and A_z are similar area fractions for flow in y and z directions then R is the coefficient that depends on the choice of coordinate system.

2.5.4 Favor Method

The fractional area method is a different method that uses another volume fractionation method which is applied to draw the geometry. Like the amount of liquid in each element of the grid to determine the position of the fluid surface.

Another partial volume can be used to define the solid surface. Essentially, it retains the volume fraction of the element not to be blocked by the solid; in a different situation, independently if one store the open or blocked part of the element, it uses the VOF technique to find a solid border through the fixed grid. Then, this data is applied to determine the wall boundary conditions that the flow must be adapted.

2.5.5 Turbulence Model

In the computation of turbulence flows, different turbulence model options are available in Flow-3D. Prandtl mixing length, one equation turbulent energy model, two equation $k-\varepsilon$ model, Renormalized group model (RNG) and large Eddy simulation model are possible options. For most applications two equation $k-\varepsilon$ models are advised for Flow-3D users (Flow 3-D user manual). Two equation $k-\varepsilon$ method was utilised in this study.

2.6 Advantages of CFD

Computer programs are rapidly developed with the advancement of technology, the analysis is now faster and easier, also with the development of computational fluid dynamics in hydraulic engineering. In principle, CFD does not replace the measurements completely but the number of experiments and the overall cost of time can be significantly reduced. Numerical models are usually cheaper and faster than physical models.They can be used for multiple-purpose at one time.

2.7 CFD Modeling Background

Ho et al. (2003) described the two and three dimensional CFD modeling of spillway behavior under rising flood levels. The results were validated using published data. Chatila and Tabbara (2004) investigated flow over an ogee spillway by using computational fluid dynamics software named ADINA to predict the free surface over an ogee spillway and thus model the flow field. They found good agreement between laboratory measurements and numerical simulations.

Gessler (2005) reviewed the hydraulic performance of the overflow spillways for a dam and simulated the flow over the two flip-bucket type spillways. The result of CFD model was validated against the physical model. He found that the result both analyses closely matched the observations made in the physical model. Erpicum et al. (2010) had studied the effect of bucket splitters on plunge pool geometry. Morales et al. (2012) studied the free flow in controlled spillway over an overflow shape by applying three-dimensional finite volume code with k – ε turbulence model and VOF method to evaluate the free surface profile. The agreement was found between the results of the physical model and numerical model. The research has shown that CFD can be used in hydraulic structures as a design tool.

A study by Tabari and Tavakoli (2016) the influence of different parameters such as the step length (L), the number of steps (Ns), the step height (h) and the discharge in the unit width (q) with energy dissipation in a simple stepped spillway were investigated. Flow-3D software was used in the analysis and the relationship between the depth of flow criticality in a stepped spillway and energy loss was evaluated. Furthermore, the finite volume method was used to solve the existing equations and $k - \varepsilon$ model was then applied to study the turbulence of flow. Based on the results, the energy dissipation decreases when the flow discharge increases and energy dissipation decreases when the number of steps increases. The results obtained were compared to other investigations, mathematical and empirical studies were conducted and finally acceptable results were obtained.

CHAPTER 3

NUMERICAL ANALYSIS

3.1 General

An ogee spillway with different end sills models, which are based on an experimental study conducted by Kanyabujinja (2015), were numerically analysed. The 3D geometry of the spillways were created and simulated by employing a commercial software called FLOW-3D. The energy dissipation was evaluated for each model with different discharges and compared with one another to find the best shape that dissipates more energy. The following section shows in detail the achievement of this work.

3.2 Geometry of the Models

The geometric and hydraulic designs of ogee spillway models used in the numerical analyses were taken from the procedures described in small Dam design by USBR (1987). The model case A has an ogee spillway with a rectangular end sill , the model case B, C, D and E with a curved end sill with different radiuses and the case F which has an inclined end sill. The dimensions of these models are almost the same (1.5 m in length, 0.6 m wide and 1.05 m high respectively) except the geometry of the end sills. Figures 3.1, 3.2 and 3.3 show the geometric dimensions of the models.

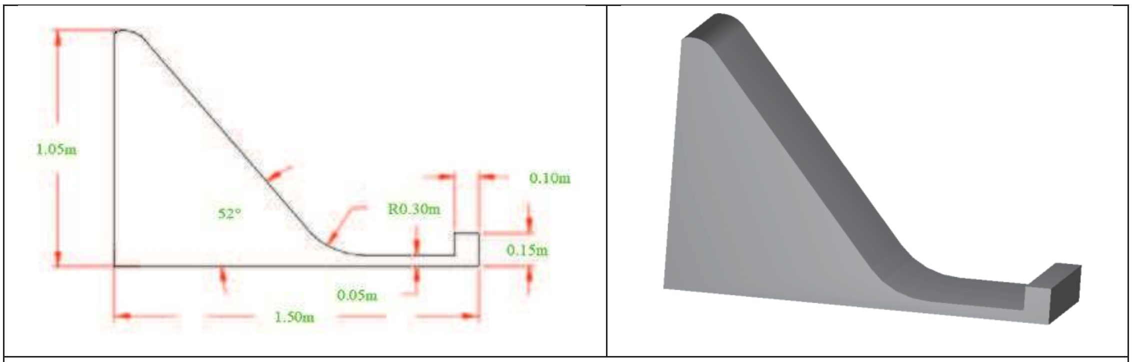

Figure 3.1 Geometric Dimensions of Case A

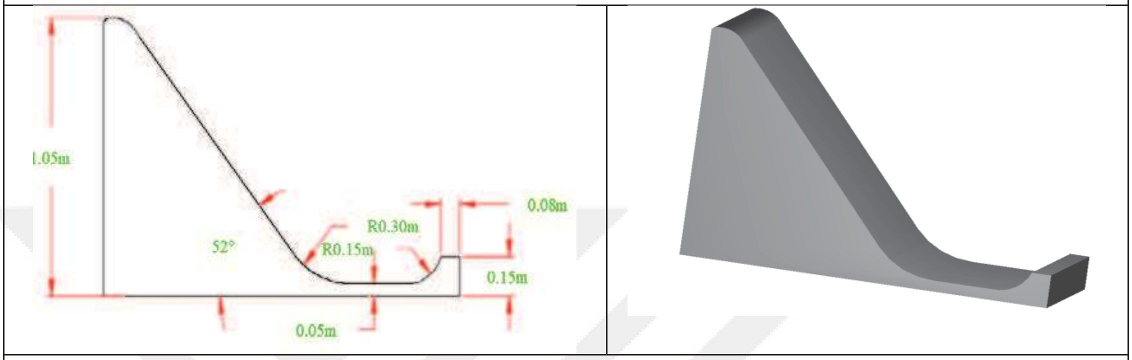

Figure 3.2 Geometric Dimensions of Case B, C, D And E

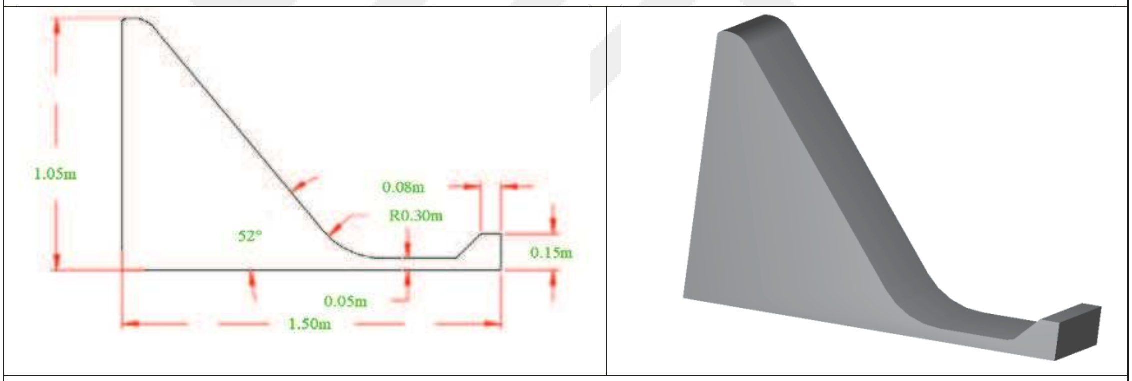

Figure 3.3 Geometric Dimensions of Case F

3.3 Numerical Modelling

Usually, there are three important steps in the procedure of CFD analyses; they are the pre-processor, the solver and the post-processor. The pre-processing in any software is the input of parameters that are required to prepare the solver step. The solver simulates the model with these parameters that is inputted in the pre-processing and the post-processor rearranges and displays the required data as output.

The numerical results depend on grid generation and its quality. In the pre-processing stage, the properties of the fluid, the boundary conditions and initial conditions should be determined. In the solver stage discretized forms of the governing equations of the fluid overall computational domain are solved. The flow parameters are calculated in each computational cell. The post-processor stage contains an amount of information for the simulated model. Moreover, in Flow-3D it means visualization of output data that is going to be displayed. The post-processing tools analyse the results and give the summary of output data in the form of 2D and 3D surface plots, vector plots, contour plots, flow lines, iso-surfaces, grid display text data outputs, geometry and several graphs can be drawn. The animation tools are also included to show dynamic results. Figure 3.4 describes different steps of CFD analysis. The rapidly development of computer technology helps to significantly reduce the time spent and expenses incurred from the physical investigation of hydraulic structures. Flow-3D package is a powerful tool used in this study.

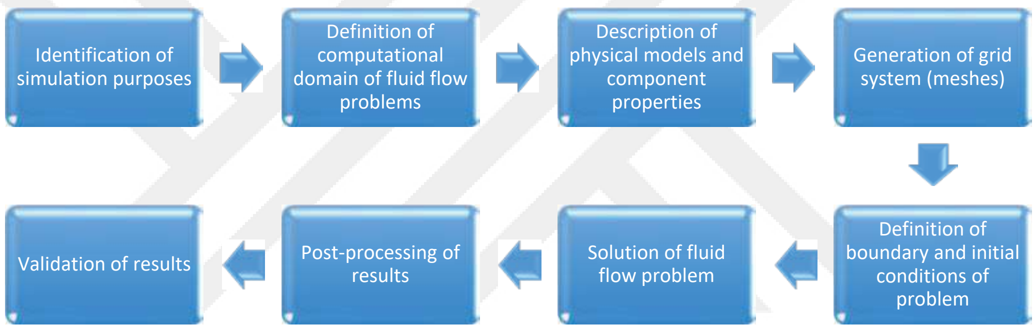

Figure 3.4 Steps of Computational Fluid Dynamic (CFD) Analysis

3.4 Brief Description of Flow-3d

The Flow-3D is used to simulate numerical models; it has a high capability on simulating free surface flows by finite difference/volume method. The software applies several features to the numerical solution of the Reynolds Averaged Navier-Stokes (RANS) equations, discretizes and solves by the continuity equation in computation cells. CFD provides accurate simulation results and uses TruVOF for the free surface. It is proven as a powerful tool for complex fluid modeling problems. To solve the RANS equation, the software uses a finite volume method. In many physical models, the basic Navier-stokes equation is selected in Flow-3D. In this study, one incompressible fluid model was applied for all discharges during the simulations.

3.5 Numerical Model Set-up

The energy dissipation was calculated for every model with a number of discharges. The software solves the fully three dimensional transient Navier-Stokes equations by volume of flow (VOF) and FAVOR method. The solver uses finite volume approximation to discretize the computational field. In simulation analyses, incompressible and free surface water with a temperature of 20^{o}C degrees was chosen.

As in other hydraulic structures; in the simulation analysis of spillways there are many physical parameters which need to be considered. The software enables several options in defining the physical parameters for the accuracy of the simulation analysis of spillways. In this study, gravity was activated by gravitational acceleration in the z-direction being set to negative 9.81 m/s^2. The viscosity and turbulence options were also selected. In the computation of turbulence flows, various turbulence models are available in Flow 3D. The two equation $k-\varepsilon$ model was employed in the analyses. The $k-\varepsilon$ model provides a reasonable approximation for many types of flow. In addition to the kinetic energy, k and the dissipation rate, ε, transport equations for turbulent diffusion, ε_T is also solved (Eq. 3.1).

$$\frac{\partial \varepsilon_T}{\partial t}+\frac{1}{V_F}\left(u\,A_x\frac{\partial \varepsilon T}{\partial x}+v\,A_y R\frac{\partial \varepsilon T}{\partial y}+w\,A_z\frac{\partial \varepsilon T}{\partial z}\right)=\frac{CDIS1.\varepsilon T}{K_T}\left(P_T+CDIS3.G_T\right)+DIff\varepsilon-CDIS2\frac{{\varepsilon_T}^2}{K_T} \qquad (3.1)$$

where $CDIS_1$, $CDIS_2$, and $CDIS_3$ are dimensionless user-adjustable parameters and have default values of 1.44, 1.92 and 0.2 respectively for the $k-\varepsilon$ model. The equation 3.2 gives the diffusion of dissipation, $DIff\varepsilon$

$$DIff\varepsilon=\frac{1}{V_F}\{\frac{\partial}{\partial x}\left(v\,\varepsilon A_x\frac{\partial \varepsilon T}{\partial x}\right)+R\frac{\partial}{\partial y}\left(v\,\varepsilon\,A_y R\frac{\partial \varepsilon T}{\partial y}\right)+\frac{\partial}{\partial z}\left(v\,\varepsilon A_z\frac{\partial \varepsilon T}{\partial z}\right)+\xi\,\frac{v\varepsilon A_x \varepsilon_T}{x} \qquad (3.2)$$

The turbulence energy dissipation rate ε_T is associated to the turbulent kinetic energy K_T described in equation 3.3.

$$\varepsilon_T=CNU\sqrt{\frac{3}{2}\frac{{K_T}^{3/2}}{TLEN}} \qquad (3.3)$$

CNU is 0.09 the default parameter, $K_T$is energy of turbulent kinetic, $TLEN$ is the scale of turbulent length

3.6 Meshing

Generating meshes (grid) for computational fluid dynamics (CFD) is neither easy nor fun. A mesh subdivides the flow domain into comparatively small parts. Each small part is called a cell, where the numerical values are calculated. Generation of mesh has a direct influence on how fast and how accurate the CFD solutions are expected to be. It is an important parameter that should be chosen carefully. In order to obtain a detailed and an adequate flow field simulation, the size of the cells should be chosen to be as small as passible. In this thesis, the mesh sizes in x, y and z directions are set to be 0.01 m.

The results can be generated in text output, in numerical data, images and animation form for presentation. Figure 3.8 illustrates the 3D and 2D computational domain for model A, which has a length of 1.5 m, a width of 0.6 m and a highth of 1.05 m. Figures 3.9 and 3.10 show the 3D and 2D computational domain for models B and C, respectively. The calculation time for all simulations was around 50 seconds, while the mesh size was fixed to be 0.01m in x, y and z directions for all models.

During the simulation stage, it is worth to note that the case A model with rectangular end sill recorded the total number of cells (active and passive) were 1571330 mesh cells. The total number of active cells were 1231411, including real cells used for solving flow equations which were 1160415, open real cells were 1153673, fully blocked real cells were 6742, external boundary cells were 70996 and inter-block boundary cell 0.

For the case model B, C, D and E model with curved end sill, the total numbers of cells (active and passive) were 1571330 mesh cells. The total numbers of active cells were 1213484, including real cells used for solving flow equations which were 1148136, open real cells were 1140078, fully blocked real cells were 6742, external boundary cells were 65348 and inter-block boundary cells were 0.

For the case F model with inclined end sill, the total number of cells (passive and active) were 1571330 mesh cells and the total number of active cells were 1212519 including real cells used for solving flow equations which were 1147191, open real cells were 1138954, fully blocked real cells were 8237, external boundary cells were 65328 and inter-block boundary cells 0.

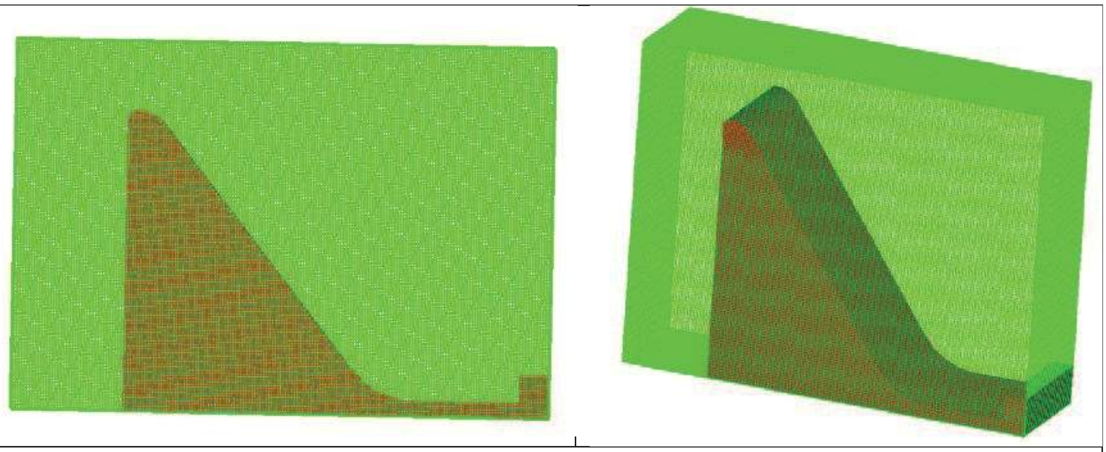

Figure 3.5 Meshing in 2D and 3D for Case A

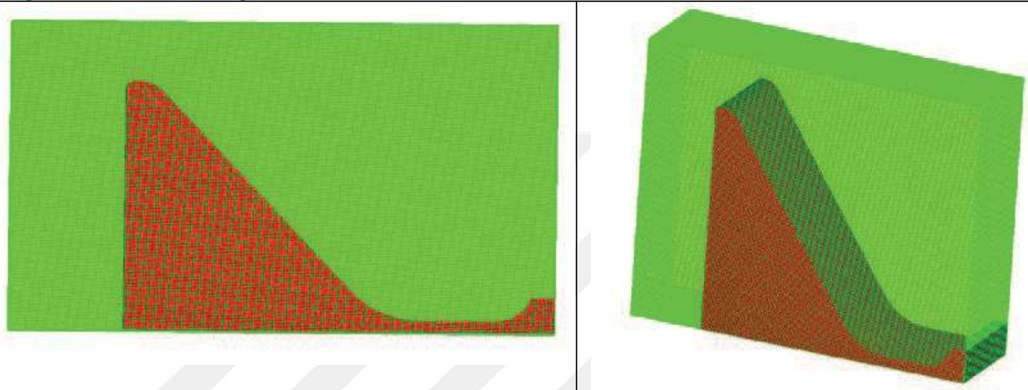

Figure 3.6 Meshing in 2D and 3D for Case B, C, D and E

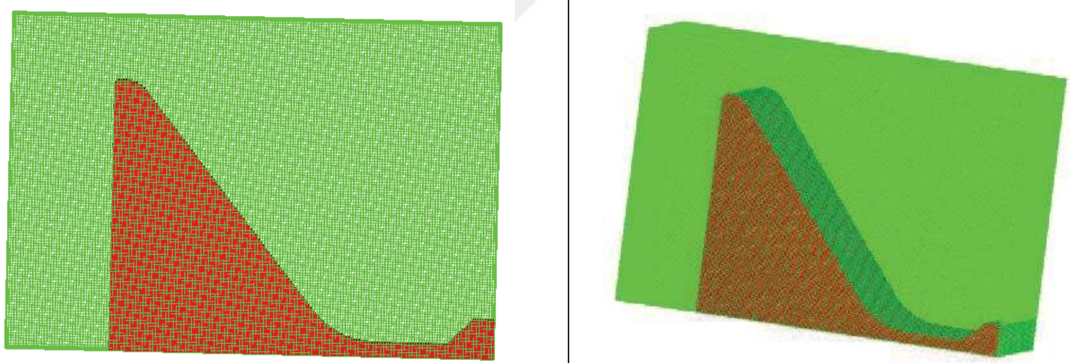

Figure 3.7 Meshing in 2D and 3D for Case F

3.7 Boundary and Initial Conditions

Navier-Stokes equation and continuity equation are solved by defining initial conditions and boundary conditions. The important role of boundary conditions is to create similar flow conditions with the physical system. The utilization of each type of boundary depends on the specific condition of the models. The boundary conditions could be defined as follows: symmetry, wall, continuative, periodic, specified pressure, specified velocity, grid overlay, outflow, wave and discharge.

Figures 3.8 specify the boundary conditions used during the simulation analyses for models A, B and C. The boundary conditions of the control volume are presented as follows: the upstream (X min) indicated the flow rate (Q) boundary condition, the downstream (X max) is the outflow (O) boundary then the bottom (Z min) is set as a wall (W) boundary condition and the top (Z max) represented the symmetry (S) boundary condition. Both (Y min) and (Y max) were selected under the symmetry boundary type for all models.

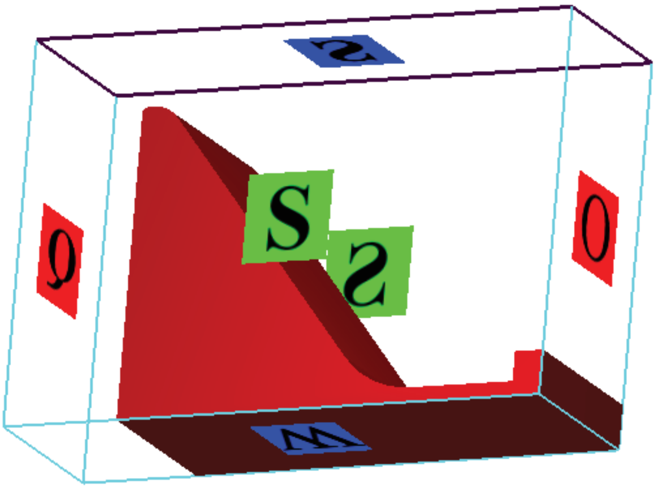

Figure 3.8 Boundary Conditions for Cases A, B, C, D, E And F

For the initial condition, a fluid area is provided within the reservoir for all models as shown in figure 3.9. The velocity of this flow of water is set to zero.

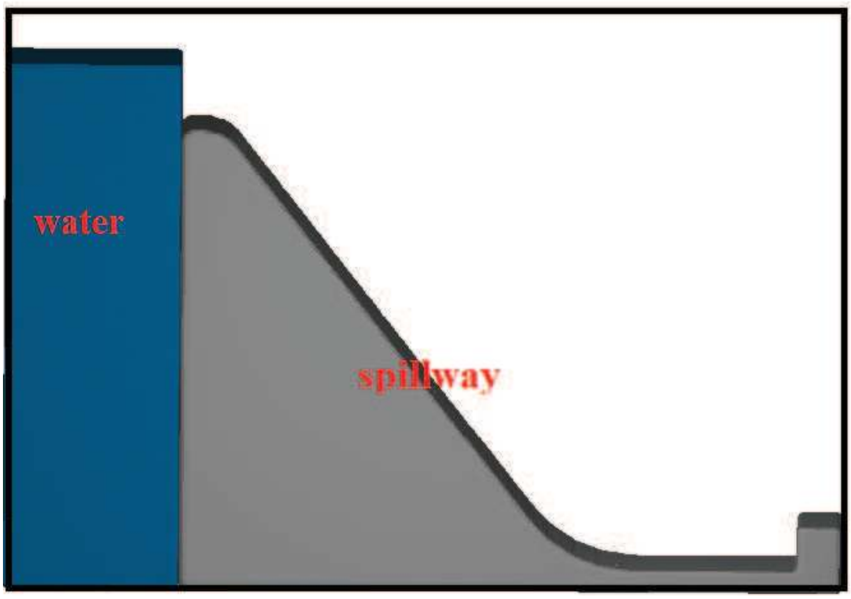

Figure 3.9 Initial Condition of Spillway

3.8 Simulation Times

The amount of time a simulation will take to reach the steady-state depends on multiple parameters. Evidently, the size and the type of problem being modelled, also the mesh resolution and block configuration has the greatest influence on simulation time. Likewise, the type of computer is another factor affecting the simulation time. In this study, all simulations were completed with HP 5.9 windows experience Index, processor Intel (R) Core (TM) i7-3770 k CPU@ 3.50 GHz 3.8 GHz. Other areas exist as well in Flow-3D that can have an impact during the simulation time, this involves the number of fluids being modelled, if the flow is supposed to be incompressible, as well as the types and amount of physics options being applied to the problem. The boundary and initial conditions implemented can also affect the simulation time. This means that a re-run is quite different from an initial simulation as it will begin with fluid flowing steadily throughout the entire domain.

3.9 Determination of Energy Dissipation

The energy losses (ΔE) means difference between upstream energy of spillway structure (E_0) and downstream (toe) of hydraulic jump location (E_1). The total energy of flow comprises of the sum of the depth of flow, velocity head at a point and is shown below.

$$\Delta E = E_0 - E_1 \tag{3.4}$$

where

$$E_1 = d_1 + \frac{{V_1}^2}{2g} \tag{3.5}$$

$$E_0 = d_0 + \frac{{V_0}^2}{2g} \tag{3.6}$$

where d is the depth of water, v is the velocity of flow and g is the gravitational acceleration (g= 9.81 m/s^2). The suffixes 0 and 1 indicate the point that energy dissipation was calculated. The percentage of energy loss in has been defined as follows:

$$\Delta E = \frac{(E_0 - E_1)}{E_0} * 100\% \tag{3.7}$$

Since the hydraulic jump is considered as an effective means for dissipating the excessive kinetic energy of flowing water at the toe of the spillway, identification of its characteristics is of importance in stilling basin designs (Yanmaz, 2006).

3.10 Similarities

3.10.1 Mechanical Similarities

A model is said to be completely similar to its full-scale prototype where the presence of scale effects are inexistent if the mechanical similarity is satisfied thereby deducing geometric, kinematic or dynamic similarity.

Geometric Similarity: The requirements of geometric similarity are focused on dimensions (sizes), where all model dimensions must be scaled by a factor λ in order to reproduce its prototype. The model can be scaled by λ , λ^2 and λ^3 for the length, area and volume respectively (Heller, 2011).

Kinematic Similarity: The kinematic similarity expresses that the particles in the motion of the model and prototype must be similar. At all times there should be a constant relationship of time, velocity, acceleration and discharge between model and prototype (Heller, 2011).

Dynamic Similarity: Heller (2011) states that dynamic similarity requires all force ratios within geometric and kinematic similarity to be identical. The most important forces when dealing with fluid dynamics are;

$$\text{inertial force} = \text{mass} * \text{acceleration} = (\rho L^3)\left(\frac{V^2}{L}\right) = \rho L^2 V^2 \quad (3.8)$$

$$\text{Gravitation force} = \text{mass} * \text{Gravitational Acceleration} = \rho L^3 g \quad (3.9)$$

$$\text{Viscous force} = \text{Dynamic viscosity} * \frac{\text{velocity}}{\text{Distance}} * \text{Area} = \mu\left(\frac{V}{L}\right)L^2 = \mu VL \quad (3.10)$$

$$\text{Surface tension force} = \text{Unit surface tension} * \text{Length} = \sigma L \quad (3.11)$$

where ρ $({kg}/{m^3})$ is the fluid density, L (m) is the length, g $({m}/{s^2})$ is the gravitational acceleration, V $({m}/{s})$ is the flow velocity, σ $({N}/{m})$ is the tensions and μ $({kg}/{m.s})$ is the dynamic viscosity.

3.10.2 Froude Similarity

The Froude similarity is verified when the ratio of gravitational and inertial forces acting on a fluid particle is equal in the model and prototype. The Froude number (Fr) is defined as;

$$Fr = \frac{V}{\sqrt{gL}} \tag{3.12}$$

where V is the flow velocity in $m/_s$, g is the gravitational acceleration ($m/_{s^2}$) and L (m) is the length.

In scale ratio of Froude model;

$$F_m = \frac{V}{\sqrt{g_m L_m}} = \frac{V}{\sqrt{g_p L_p}} = F_p \tag{3.13}$$

with $g_m = g_p = g$ not scaled L_m and L_p are length of model and prototype respectively

$$L_p = \lambda L_m \tag{3.14}$$

$$F_m = \frac{V_m}{(gL_m)^{1/2}} = \frac{V_p}{(gL_p)^{1/2}} = F_p$$

$$\frac{V_m}{(gL_m)^{1/2}} = \frac{V_m}{(g\lambda L_m)^{1/2}} \tag{3.15}$$

It is reduced to

$$V_m = \frac{V_p}{\lambda^{1/2}} \tag{3.16}$$

and

$$V_p = \lambda^{1/2} V_m \tag{3.17}$$

$\lambda^{1/2}$ is the required to upscale Froude model velocities.

The ratio of flow between model and prototype can be calculated as:

$$\frac{V_m}{(gL_m)^{1/2}} = \frac{V_p}{(gL_p)^{1/2}} \Longrightarrow \frac{V_m}{V_P} = \sqrt{\frac{L_m}{L_p}} \tag{3.18}$$

$$\frac{Q_m}{Q_p} = \frac{A_m V_m}{A_p V_p} = \frac{{L_m}^2}{{L_p}^2} \sqrt{\frac{L_m}{L_p}} \tag{3.19}$$

$$Q_m = Q_P . 10^{-5} \tag{3.20}$$

The design discharge of prototype can be calculated from the model by using the above formulas, the discharges of the prototypes were found to be as follows; While Q_{model} was 60 l/s, 75 l/s and 89 l/s for these models $Q_{prototype}$ was calculated to be 6000 m^3/s, 7500 m^3/s and 8900 m^3/s.

CHAPTER 4

RESULTS AND DISCUSSION

4.1 Introduction

The amount of energy that can be dissipated by six different end sill designs of an ogee spillway is analysed and outcomes are compared with one another. The aim of this investigation is to numerically assess the optimum end sill design, from energy loss point of view. A number of flow discharges were employed in the simulation analysis. The effect of flow discharge and the influence of the end sill design on the energy dissipation rate for each single model were observed. 36 simulations scenarios were carried out with discharges of 51, 60, 75, 89, 95 and 120 liters per second. The simulations were performed in a time period of 66 heures.

4.2 Simulation Analysis

4.2.1 Energy Dissipation Rate for Case A

The rate of energy dissipation by case A, which has a rectangular end sill shape (Figure 4.1) was numerically simulated by six different cases of discharge. The total amount of dissipated energy was estimated by taking the differences in the energy of water flow at two specific sections on the spillway. The upstream section was selected to be the peak of the spillway while the downstream section was chosen to be after the location of the hydraulic jump. The flow of water over the spillway and occurrence of hydraulic jump are shown step by step in figure 4.1. The energy dissipation results obtained for each discharge are given in table 4.1 and presented in figure 4.2. It can be seen that the energy losses were found to be 67%, 65%, 64%, 61%, 56% and 55% for flow discharges of 51, 60, 75, 89, 95 and 120 l/s. As the flow discharge increased, the rate of energy dissipation was perceived to be decreased in model case A.

Table 4.1 Energy Dissipation for Case A

Model	Discharge (l/s)	Dissipated Energy (%)
Case A	51	67
	60	65
	75	64
	89	61
	95	56
	120	55

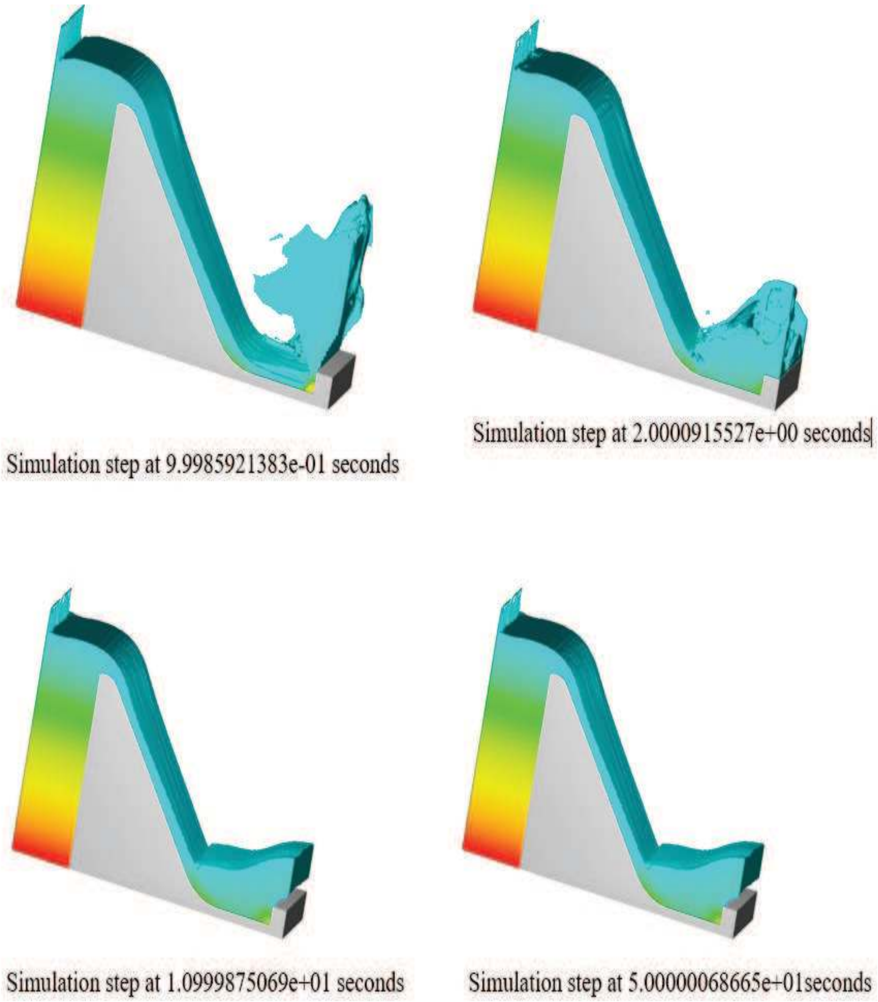

Figure 4.1 Simulation Steps for the Case A

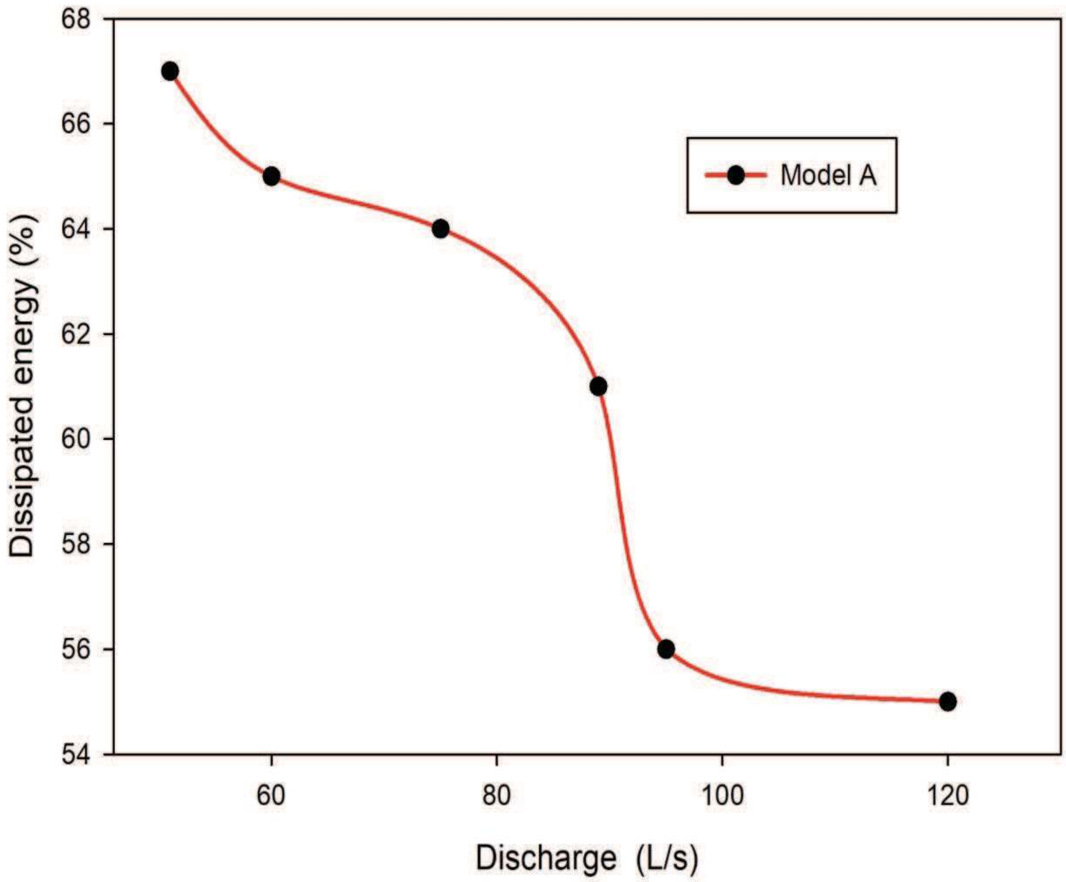

Figure 4.2 Energy Dissipation Rate for Case A

4.2.2 Energy Dissipation Rate for Case B

In the simulation of case B, the energy dissipation values with the curved end sill downstream and a radius of 0.15 m were found to be 72%, 69%, 67,4%, 63%, 62% and 58,1% for 51, 60, 75, 89, 95 and 120 ls^{-1} of discharge, respectively. Therefore, by increasing the flow rate, the energy dissipation rate decrease. The hydraulic jumps' occurrences are displayed in Figure 4.3. The energy dissipation rates were recorded and tabulated in Table 4.2 and presented in Figure 4.4.

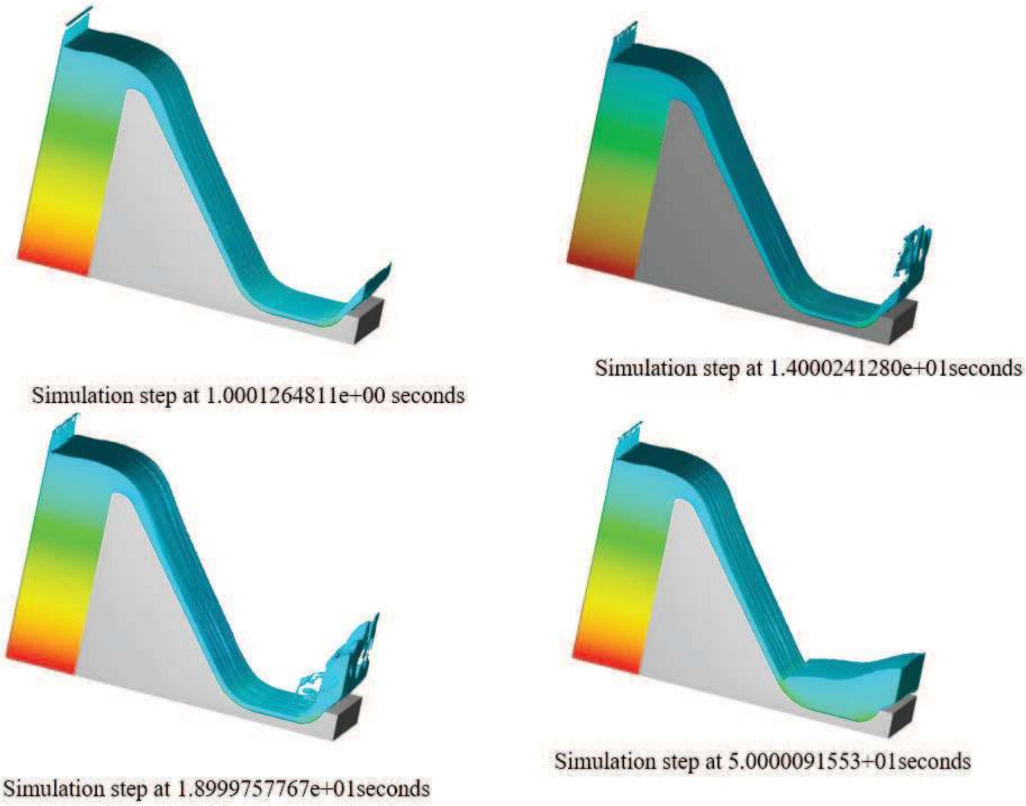

Figure 4.3 Simulation Steps for Case B

Table 4.2 Energy Dissipation for Case B

Model	Discharge (l/s)	Dissipated Energy (%)
Case B	51	72
	60	69
	75	67,4
	89	63
	95	62
	120	58,1

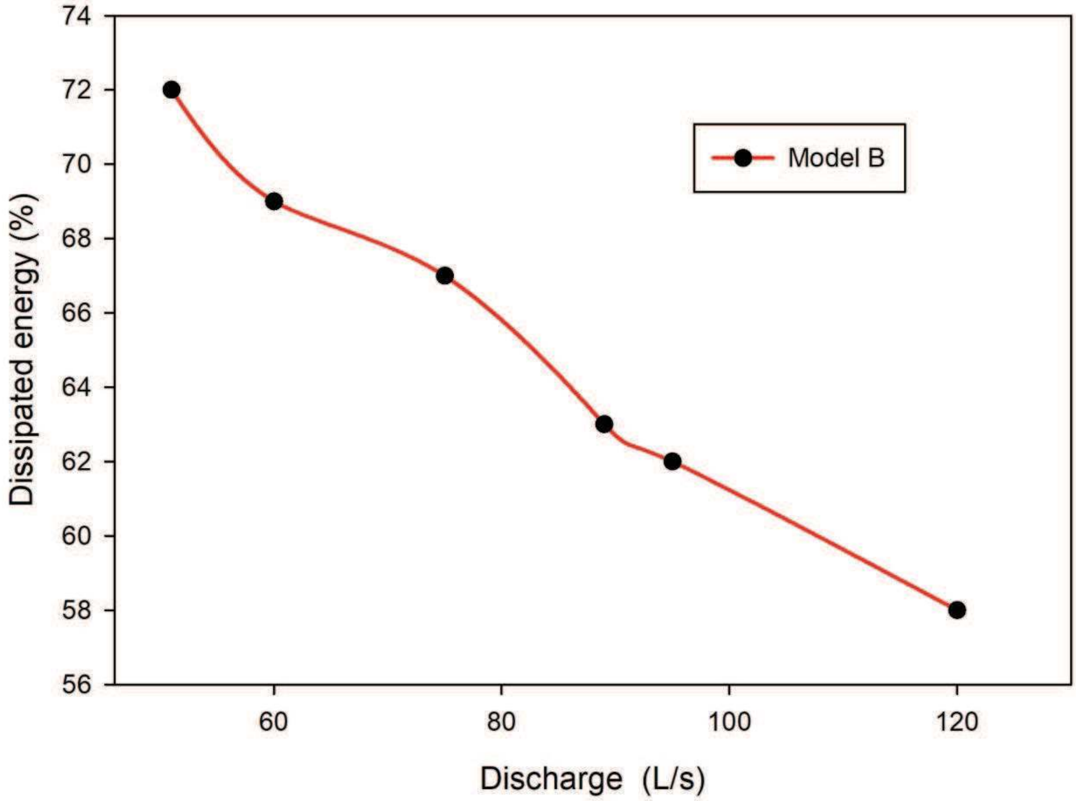

Figure 4.4 CFD Result for Case B

4.2.3 Energy Dissipation Rate for Case C

During the simulation of case C which has a curved end sill downstream with radius of 0.10 meter , the energy dissipated were found to be 73%, 69.3%, 68.4%, 64%, 63% and 59% for 51, 60, 75, 89, 95 and 120 ls^{-1} as discharge, respectively. Therefore, by increasing the flow rate, the energy dissipation decrease as well. The hydraulic jumps' occurrences are displayed in Figure 4.5. The energy dissipation rates were recorded and tabulated in Table 4.3 and shown in Figure 4.6.

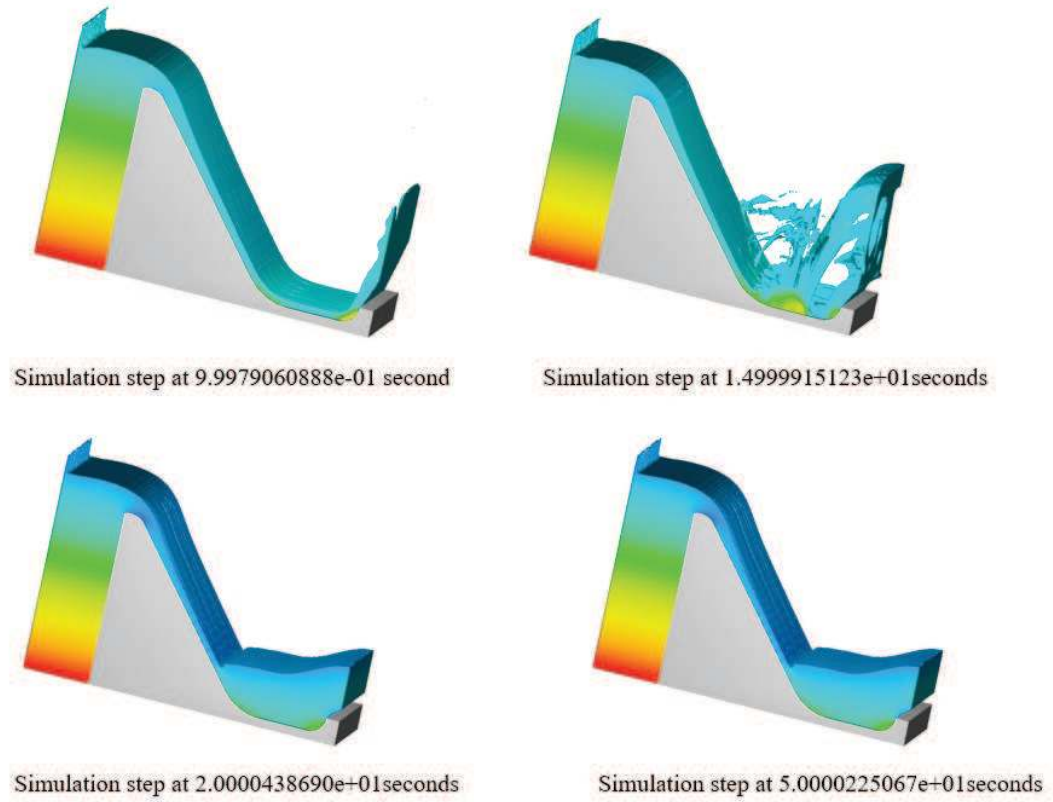

Figure 4.5 Simulation Steps for Case C

Table 4.3 Energy Dissipation for Case **C**

Model	Discharge (l/s)	Dissipated Energy (%)
Case C	51	73
	60	69.3
	75	68.4
	89	64
	95	63
	120	59

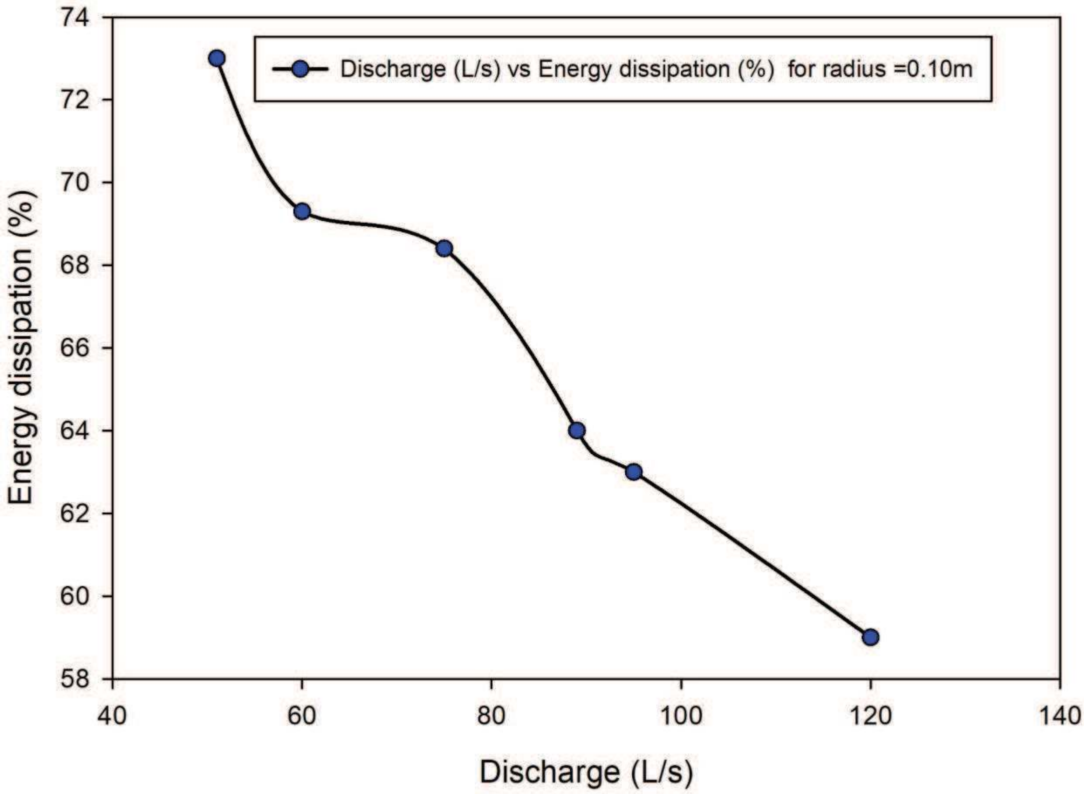

Figure 4.6. Energy Dissipation Rate for Case C

4.2.4 Energy Dissipation Rate for Case D

In the simulation of case D, the energy dissipation values with the curved end sill downstream and a radius of 0.18 m were found to be 21%, 18%, 16%, 16%, 15% and 14.1% for 51, 60, 75, 89, 95 and 120 ls^{-1} as discharge, respectively. Figure 4.7 shows the test scenarios for this model.

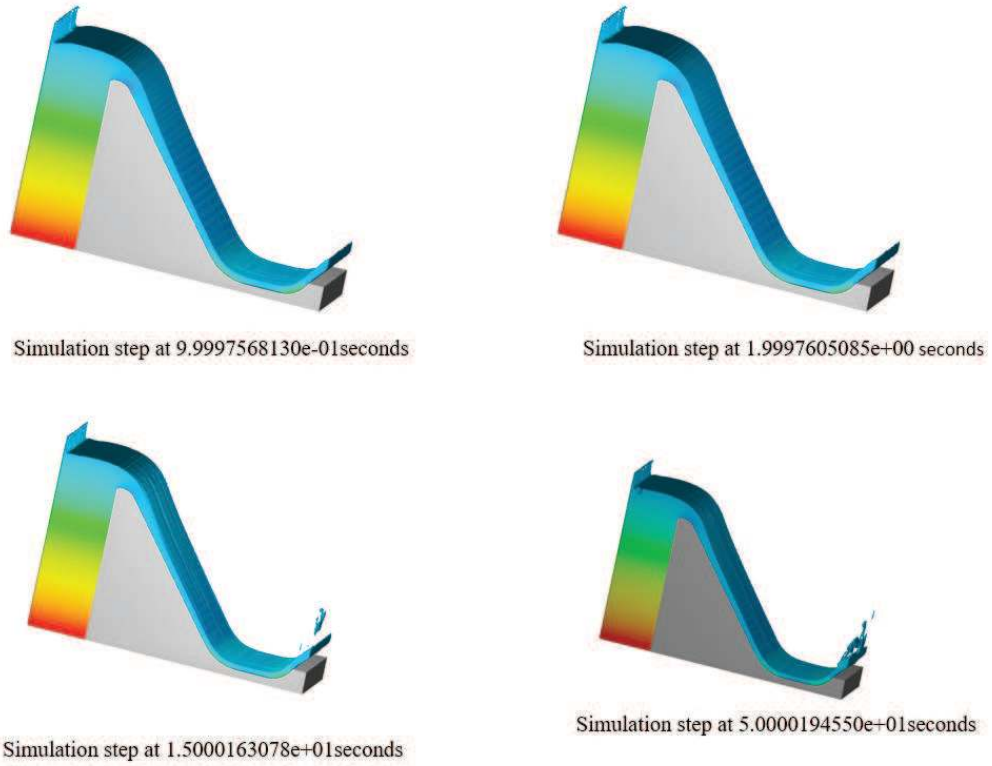

Figure 4.7 Simulation Steps for Case D

It is important to mention that for the radius of 0.18, the results revealed the lack of the hydraulic jump formation at downstream. In addition, not only the dissipation of energy was very low but also spillway end sill radius dependent. The Table 4.4 and Figure 4.8 summarized the results of this case model.

Table 4.4 Energy Dissipation for Case D

Model	Discharge (l/s)	Dissipated Energy (%)
Case D	51	21
	60	18
	75	16
	89	16
	95	15
	120	14.1

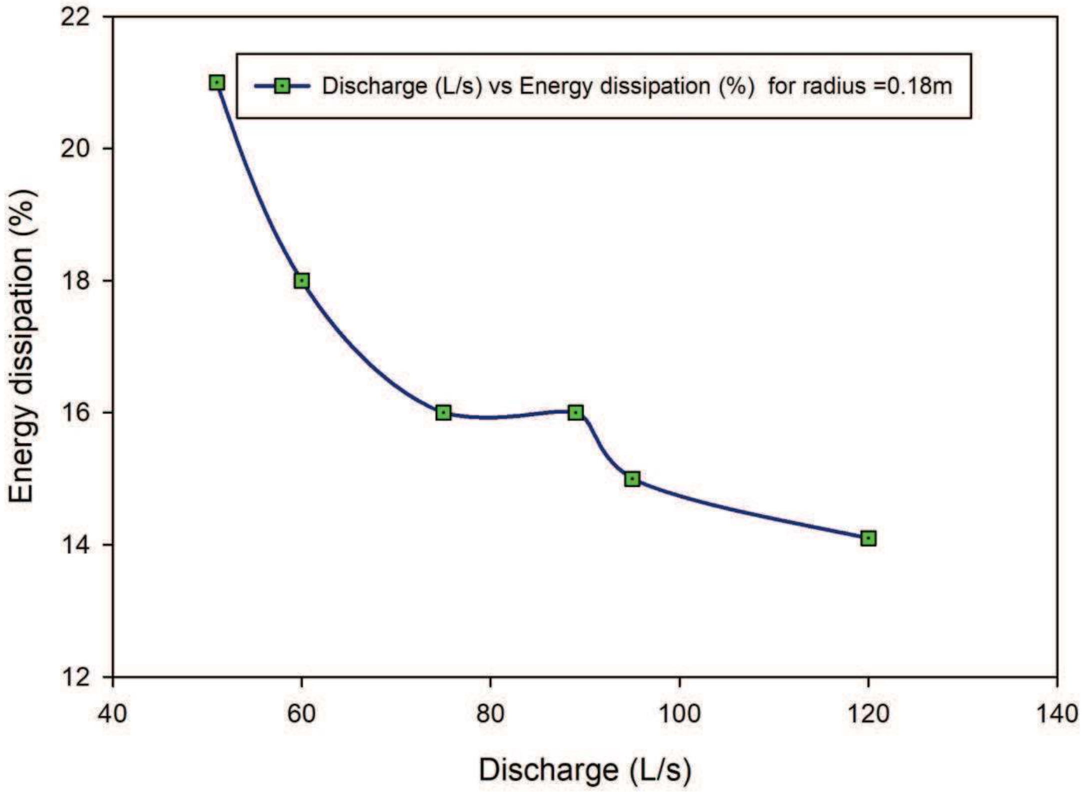

Figure 4.8. Energy Dissipation Rate for Case D

4.2.5 Energy Dissipation Rate for Case E

For this case model which has a curved end sill with radius of 0.20 m at downstream. The results were found to be 19%, 18%, 17%, 16%, 14% and 13.4% for 51, 60, 75, 89, 95 and 120 ls^{-1} as discharge, respectively. Figure 4.9 shows the test scenarios for this model.

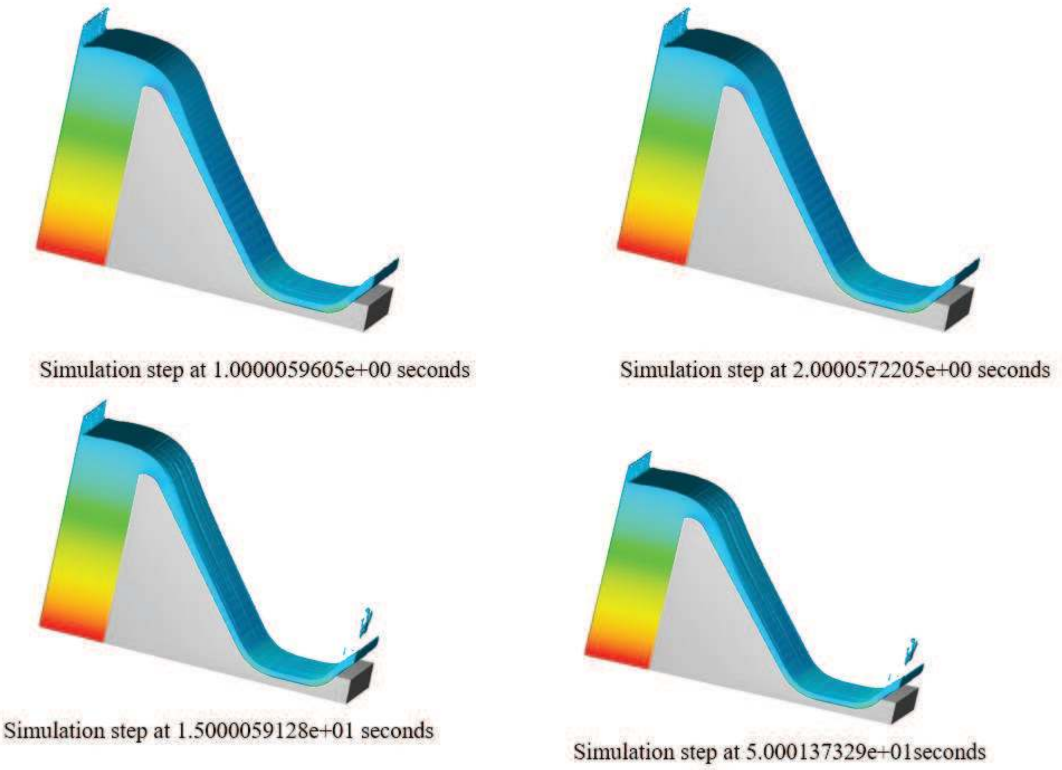

Figure 4.9 Simulation Steps for Case E

The results of the investigation demonstrated that the energy dissipation decreases as the discharge increases. Thus, energy dissipation is inversely proportional to the water discharge. Furthermore, the hydraulic jump did not occur and water is flowing with a higher velocity. The Table 4.5 and Figure 4.10 tabulate the results of this case model.

Table 4.4 Energy Dissipation for Case E

Model	Discharge (l/s)	Dissipated Energy (%)
Case E	51	19
	60	18
	75	17
	89	16
	95	14
	120	13.4

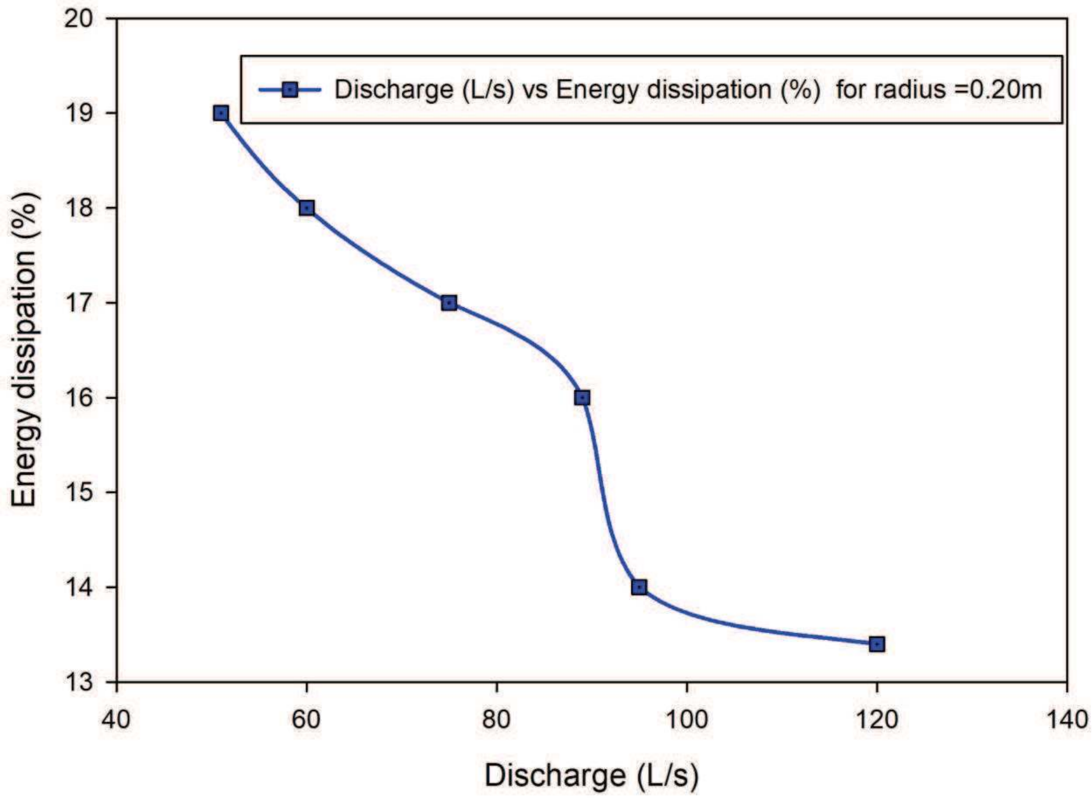

Figure 4.10. Energy Dissipation Rate for Case E

4.2.6 Energy Dissipation Rate for Case F

For this case of model with inclined end sill, the CFD results are presented in Table 4.6 and Figure 4.11. It can be said that the hydraulic jump did not occur. The velocity remained high at the downstream. The dissipation of energy is very low and insignificant regarding its form. Figure 4.10 show the simulation step of this model.

Table 4.4 Energy dissipation for case F

Model	Discharge (l/s)	Dissipated Energy (%)
Case F	51	37
	60	27
	75	25
	89	21
	95	18
	120	17

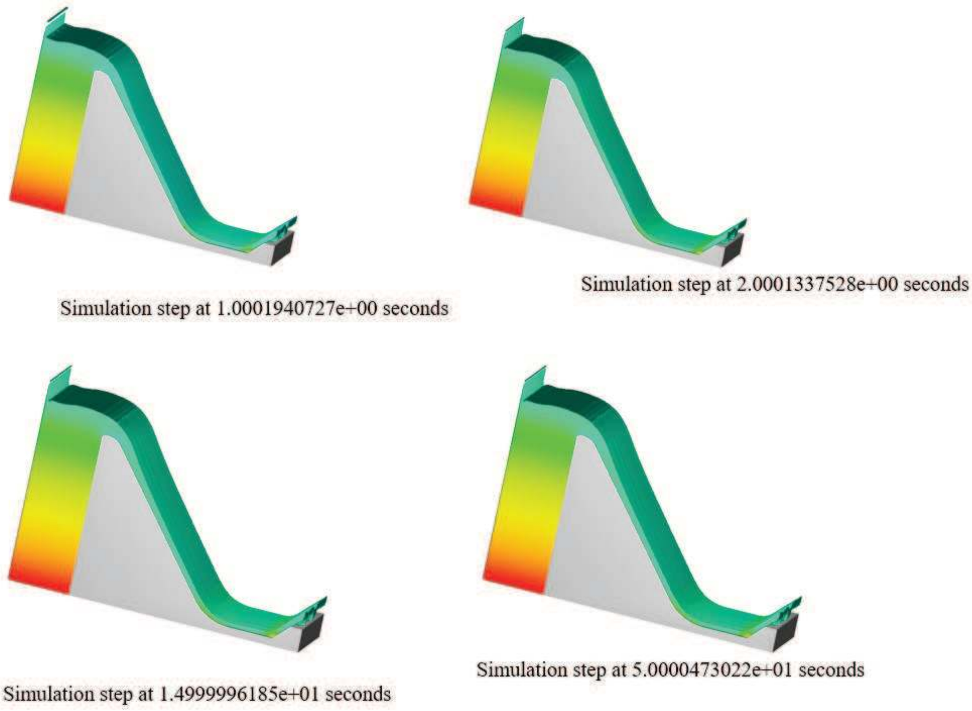

Figure 4.10 Simulation Steps for Case F

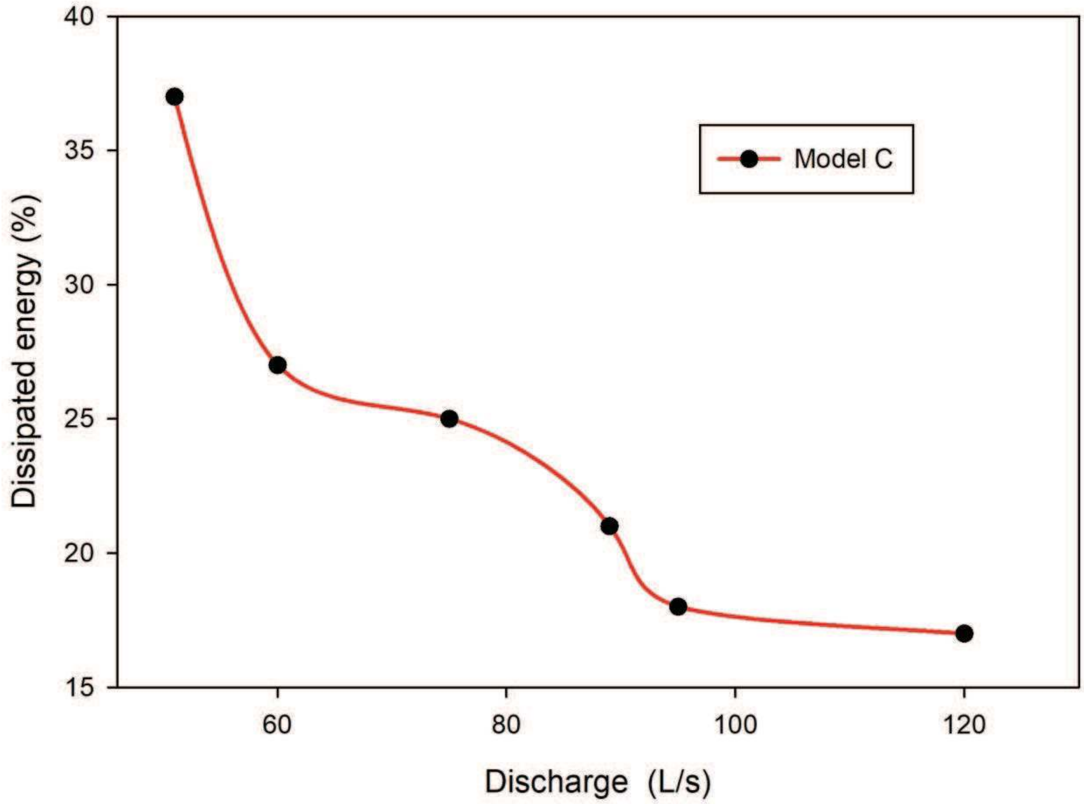

Figure 4.11 Energy Dissipation Rate for Case F

4.3 Observation of Parameters in CFD

4.3.1 Froude Number Distribution

The Froude number is a parameter that should be verified if the water flow is converted from supercritical to subcritical for the dissipation of energy. When the hydraulic jump takes place, the Froude number has to be less than 1. Figure 4.12 shows the 2D simulation for the respective model with different changes of Froude values before and after the hydraulic jump.

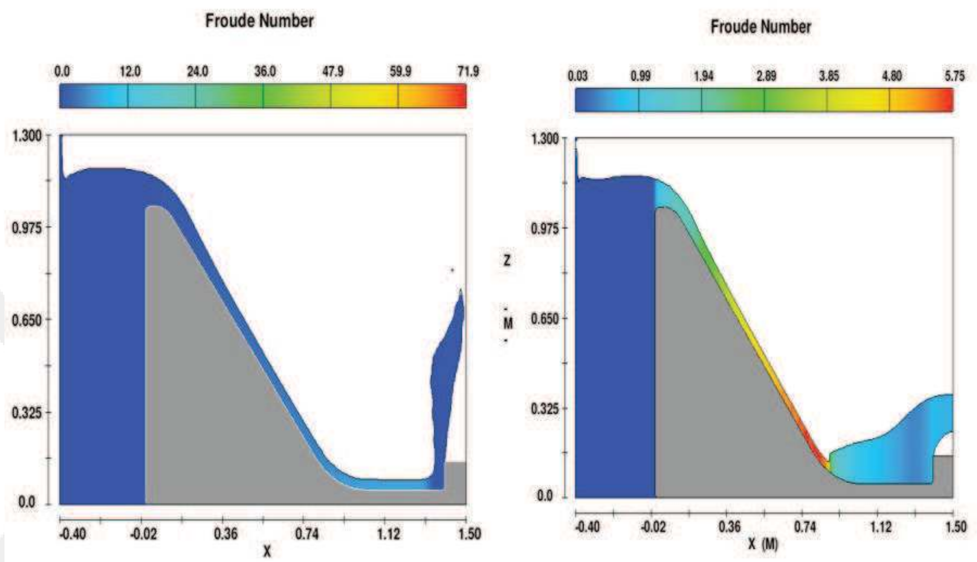

Figure 4.12 Froude Number Distributions before the Jump for Case A

4.3.2 Velocity Distribution.

Due to high velocities, erosion of the spillway face may occur for the given flow condition. In fact, it was noted that a large velocity reduction occured at the end of the basin. Thus, high energy dissipation takes place in the basin for the hydraulic jump. Figure 4.13 shows the velocity distribution throughout the simulation domain before and after the hydraulic jump.

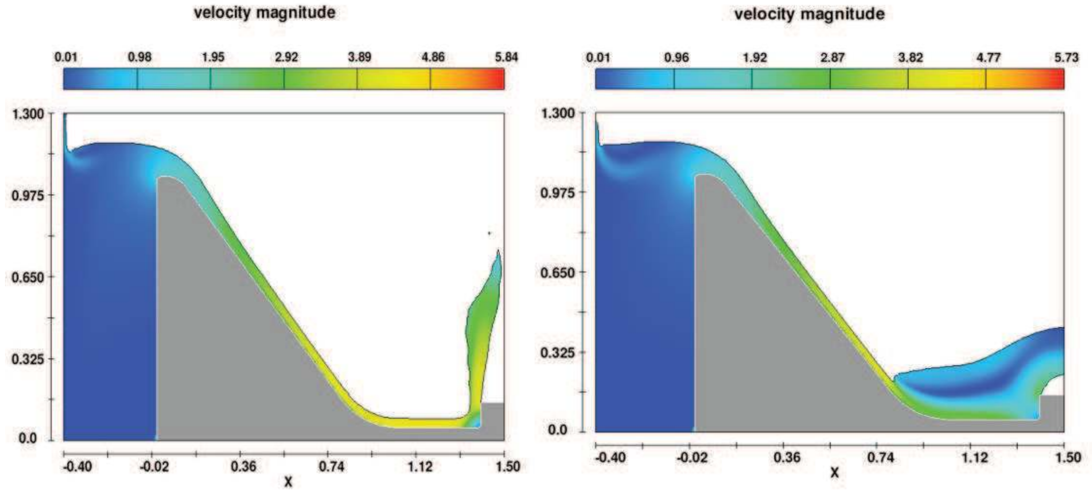

Figure 4.13 Velocity Magnitudes before and after the Jump for Case A

In comparison, of each model, it is observed that case C with the curved end sill and small radius (0.10 m) has more energy dissipation ratio, better operation and more efficient than the others. In every discharge, this model proved to be the best. Furthermore, in different cases, energy loss changes have a different process in comparison to discharge, but according to most graphs, most loss occurs for low discharge and also in the higher discharges energy loss decreases. The summary graph in figure 4.14 shows overall system losses of these models.

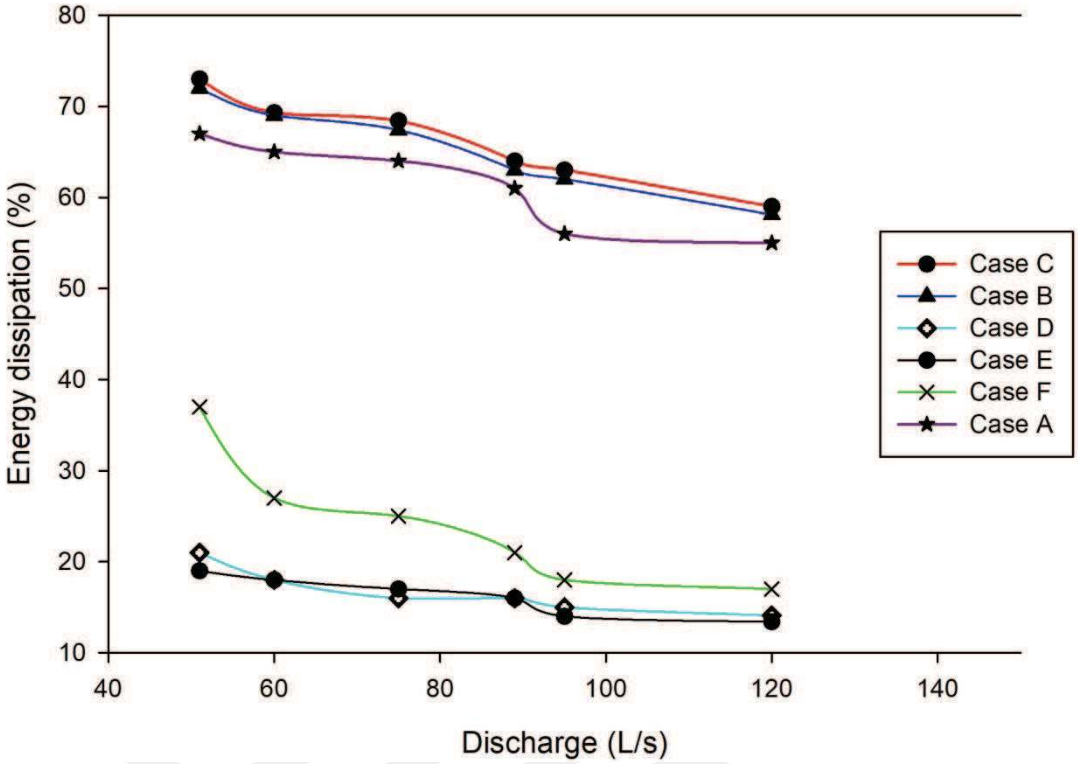

Figure 4.14 Overall System Losses in Flow-3D

CHAPTER 5

CONCLUSION

The numerical analysis developed with computer technology can be an appropriate and effective tool for analyzing flow over spillways. it can provide additional information that physical may not in the model tests. The investigation of energy dissipation over an overflow spillway was numerically simulated with a commercial software Flow-3D. The volume of flow (VOF) and $(k-\varepsilon)$ turbulent model were applied in the numerical model.

For 3D modelling, the orthogonal mesh was selected in x, y and z-direction, the mesh grid is equal to 0.01 m.

The major findings of the numerical result of this research can be summarized that model case C is more efficient for energy dissipation than others; it dissipates more energy in all cases of discharge. It is worth to note that the curvature radius of the end sill for the curved cases should not be large, because it causes the reduction of the energy operation. In addition, the results of the investigation demonstrated that the energy dissipation decreases as the discharge increases. Thus, energy dissipation is inversely proportional to the water discharge.

compare to the case E with inclined end sill, it can be concluded that the hydraulic jump did not occur in this form of model, the velocity remained high for all cases of discharge and the energy loss was insignificantregarding its form.

Future Suggestion

The present study has provided a survey of the CFD modeling of ogee spillways. Based on these concluding observations, the following suggestions are made:

- This study attempted to investigate the uncontrolled overflow spillway hydraulics with Flow-3D software. The same validation is suggested for a controlled overflow spillway in order to evaluate the use of this software in the design and testing processes of this particular type;

- Other types of turbulence model apart from The standard $(k - \varepsilon)$ turbulent model and Volume of Flow model is recommended;
- During the simulation, for the case F model the hydraulic jump did not occur and the velocity remained high at the downstream.

REFERENCES

AASHTO. American Association of State Highway and Transportation officials. 2014. *Drainage Manual, Chapter 11 Energy Dissipators.* Washington, DC : Technical Committee on Hydrology and Hydraulics.

Bombardelli F A, Meireles I and Matos J. 2011. Laboratory measurements and multi-block numerical simulation of the mean flow and turbulence in the non-aerated skimming flow region of steep stepped spillways, *Journal of Environmental Fluid Mechanics*. 11, 263-288.

Brown K W, Savage B and Paxson S G 2012. Revisiting Spillway discharge coefficients for several weir shapes. *32nd Annual USSD conference: Innovative Dam and Levee Design and Construction for Sustainable Water Management* 1317-1335. New Orleans, Lousiana: United States Society on Dams (USSD).

Brater F E, King W H, Lindell J and Wei Y C 1996. *Handbook of Hydraulics.* New York: MC Graw - Hill.

Chatila J, Tabbara M. 2004 Computational modeling of flow over ogee spillway. Comput struct; 82, 1805-12

Chadwick A, Morfett J, and Borthwick M. 2004. *Hydraulics in Civil and Environmental Engineering.* New York: Spon Press.

Chanel, P.G. 2008. "An evaluation of computational fluid dynamics for spillways", Thesis (MSC), University of Manitoba, Canada, 11-23.

Daneshkhah A and Vosoughifar. 2012 A solution of Flow Field Equations to investigate the Best Turbulent Model of Flow over a Standard Ogee Spillway in Finite Volume Method. *The First International Conference on Dams & Hydropower.*

Dr. Pierre J. 2014. Weirs across an open channel, CIVE 401 – Hydraulic Engineering.

Dhaktode Asaram, Gatne Deepamkar, Gurjeet Sıngh, Kasabe Vıshal, Kasawa Akshay, Energy Dissipation by using different Slopes of Ogee Spillway, International Journal of Engineering Research and General Science Volume 4, Issue 3, May-June, 2016 ISSN 2091-2730, 18-22

Erpicum S, Archambeau P, Dewals B and Pirotton M. 2010, Experimental investigation of the effect of flip Bucket Splitters on Plunge Pool Geometry, WasserWirtschaft, 108-110.

Federal Highway Administration, 1983. Hydraulic Design of Energy Dissipators for Culverts and Channels, s.l.: U.S. Department of Transportation.

Flow Science Inc. 2012. FLOW-3Dv10-1-user-manual, flow science, inc Santa Fe

Gessler D. 2005. CFD Modelling of Spillway performance, EWRI 2005: Impacts of global climate change. *In Proceedings of the World Water and Environmental Resources Congress.* Anchorage, Alaska: American Society of Civil Engineers.

Hager W H 1985. B-jumps at abrupt channel drops, *Journal of hydraulic Engineering*, **111(5)**, 861-866.

Ho H, Boyes K, Donohoo S and Cooper B. 2003. "Numerical flow analysis for spillways", Proc., 43rd ANCOLD Conf., Hobart, Tasmania, 24-29 .

Heller V. 2011. Scale effects in physical hydraulic engineering models. *Journal of Hydraulic Research,* 49(3), 293-306.

ICOLD. 2012. Complementary Use of Physical and Numerical Modelling Techniques in Spillway Design Refinement. *ICOLD, 24th Congress* 55-76. Kyoto: ICOLD.

Johnson M C and Savage B M. 2006. Physical and numerical comparison of flow over ogee spillway in the presence of Tailwater, *journal hydraulic Engineering*, 132, No. 12, 1353-1357.

Kanyabujinja N P. 2015. CFD modeling of ogee spillway hydraulics and comparison with physical model tests (*Doctoral dissertation, Stellenbosch: Stellenbosch University*).

Khatsura R M 2005. "hydraulics of spillways and energy dissipators", 1st Ed., Marcel Dekker, New York, USA

Khosro Morovati, Afshin Eghbalzadeh, Saba Soori, Numerical Study of Energy Dissipation of Pooled Stepped Spillways, Civil Engineering Journal . 2, No. 5, May, 2016

Kjellesvig H. 1996. Numerical Modelling of Flow over a Spillway. *Hydroinformatics- 96.*

Kumcu S Y. 2017. Investigation of flow over spillway modeling and comparison between experimental data and CFD analysis, *KSCE Journal of Civil Engineering,* 21, No 3, 994-1003.

Maynord, T. S. 1985. *General Spillway investigation.* Washington D.C: Department of The Army - Waterways Experiment STation-Corps of Engineers.

Murphy T. 1973 Dec. Spillway Crest Design. Vicksburg, U.S.A: U.S Army Engineer Waterways Experiment Station.

Mohammad Rezapour Tabari M, Tavakoli S. 2016. Effects of Stepped Spillway Geometry on Flow Pattern and Energy Dissipation, *Arabian Journal for Science & Engineering (Springer Science & Business Media BV)*, **41**(4).

Morales V, Tokyay T E, Garcia M. 2012, June. Numerical modeling of ogee crest spillway and tainter gate structure of a diversion dam on Canar River, Ecuador, *In XIX International Conference on Water Resources*, University of Illinois at Urbana-Champaign.

Nichols B D and Hirt C W. 1975, Methods for Calculating Multi-Dimensional, Transient Free Surface Flows Past Bodies, *Proc. First Intern. Conf. Num. Ship Hydrodynamics, Gaithersburg, ML*, Oct. 20-23, 1975

Rajaratnam N and Subramanya K. 1968. Hydraulic jumps below abrupt symmetrical expansions, *Journal of the Hydraulics Division*.

Reclamation, U. B. O. 1987. Design of small dams. *Water Resources Technical Publication*, 860.

Russell S O D. 2005. Hydraulics of spillways and energy dissipators1, *Canadian Journal of Civil Engineering*, **32(2)**, 461.

Savage M and Johnson M. 2001. Flow over Ogee Spillway: Physical and Numerical model Case Study. *Journal of Hydraulic Engineering 127(8)*, 640-649.

Sharif N and Ravori R A. 2014 experimental and numerical study of the effect of flow separation on dissipating energy in compound Bucket. *2013 2nd International Conference on Civil Engineering (ICCEN 2013). 334-338*

Shanmukha 2016. Water resource engineering 2. " types of weirs and flow over weirs" *Civil engineering WordPress update.*

U.S.B.R. 1973. *Design of Small Dams.* United States Department of Interior - Bureau of Reclamation.

USACE, U., 1992. Army Corps of Engineers. *CECW-ED-D Engineer Manual 1110-2-1603*.

Versteeg H and Malalasekera W. 2007. *An introduction to Computational Fluid Dynamics: The finite volume method.* England: Prentice Hall.

Yanmaz A M 2006. Applied water resources engineering, department of civil engineering Middle East Technique University, Third edition